2013-01-28

Removal of Naphthenic Acid from Water Using Biomass-based Activated Carbon

Iranmanesh, Sobhan

UNIVERSITY OF CALGARY

Removal of Naphthenic Acid from Water Using Biomass-based Activated Carbon

by

Sobhan Iranmanesh

A THESIS

SUBMITTED TO THE FACULTY OF GRADUATE STUDIES

IN PARTIAL FULFILMENT OF THE REQUIREMENTS FOR THE

DEGREE OF DEGREE OF MASTER OF SCIENCE

Chemical and Petroleum Engineering

CALGARY, ALBERTA

January, 2013

UNIVERSITY OF CALGARY

FACULTY OF GRADUATE STUDIES

The undersigned certify that they have read, and recommend to the Faculty of Graduate Studies for acceptance, a thesis entitled "Removal of Naphthenic Acid from Water Using Biomass-based Activated Carbon " submitted by Sobhan Iranmanesh in partial fulfilment of the requirements of the degree of Master of Science.

_____

Supervisor, Dr. Thomas Grant Harding,
Department of Chemical and Petroleum Engineering

_____

Co- Supervisor, Dr. Jalal Abedi
Department of Chemical and Petroleum Engineering

_____

Co- Supervisor, Dr. David Layzell
Department of Biological Sciences

_____

Dr. Alex Andre Hugo De Visscher
Department of Chemical and Petroleum Engineering

_____

Dr. Michael William Foley
Department of Department of Chemical and Petroleum Engineering

_____

Dr. Angus Chu
Department of Department of Civil Engineering

_____

Date

Abstract

In oil sands mining operations, water is an essential ingredient of the extraction process, however, it becomes contaminated through contact with bitumen at high temperature, and ultimately ends up in tailings ponds. Through repeated recycling of produced water, concentration of contaminants increases over time. Similar contamination of water occurs in oil sands in-situ recovery operations where high pressure saturated steam is commonly used to contact bitumen in the reservoir. Some of the most troublesome of the contaminants found in the produced water are naphthenic acids, naturally occurring compounds in bitumen. Naphthenic acids are a mixture of alkyl-substituted acyclic and cycloaliphatic carboxylic acids. Studies have shown that the concentration of naphthenic acids in tailings ponds and produced water from in-situ recovery operations is substantial and that they are corrosive and toxic making their removal from water crucially important. In addition, the presence of dissolved organic compounds in tailings pond water is thought to contribute, through bacterial degradation, to the emission of methane from the ponds into the atmosphere, methane being one of the most potent greenhouse gasses.

Several methods have been reported for removing naphthenic acids from water, such as catalytic reactions, membrane separation, microbial reaction and adsorption. In this work, the removal of naphthenic acids by adsorption using activated carbon was investigated since among a variety of adsorbents, activated carbon is considered to be highly effective. Sawdust was selected as the raw material for producing activated carbon due to its abundance and anticipated low cost. In addition, biomass-based activated carbon can play a role as a carbon sink so it can contribute to reducing the carbon emission footprint of oil sands operations.

The methods employed in this work for producing activated carbon from sawdust were physical activation using carbon dioxide (CO_2) and chemical activation using phosphoric acid (H_3PO_4). For comparison, a commercially activated carbon was also used. The physically activated carbons were found to have lower surface area than the chemically activated carbon. In biochar production, the carbonization temperature showed the strongest effect on yield of produced biochars. Heating rate and activation time were ranked second and third respectively. Generally a yield of around 20-30% is expected during the production of biochar from sawdust. During physical activation of the biochar, activation temperature was shown to be the most important factor affecting the surface area of the activated carbon and an optimum activation temperature of 825 °C was determined. The Langmuir Isotherm provided the best fit of experimental data for the physically activated carbons suggesting mono-layer adsorption. The Sip isotherm provided the best fit to the data for the chemically activated carbon.

Naphthenic acid adsorption tests were done at different initial concentrations, in order to obtain the isotherm for each activated carbon. In the adsorption tests, the chemically activated carbon showed greater uptake of naphthenic acid, which can be attributed to the higher surface area and increased mesopore size. It was observed that both the chemically and physically activated carbons had greater naphthenic acid uptake than the commercially activated carbon. A removal range between 60-90% of total organic carbon (TOC) was achieved using ACs produced in this study for different concentrations of contaminants.

Acknowledgements

I would like to express my sincere gratitude to my supervisor Dr. Thomas Harding and my co-supervisors Drs. Jalal Abedi and David Layzell for their support, advice, patience, motivation and invaluable guidance. They have been a constant source of inspiration, and it has truly been a great privilege for me to work with them. Without their support and help, this work could not have been accomplished. Again, I highly appreciate everything they have done and taught me.

I would also like to express my gratitude to Dr. Azad for all of her help in Isfahan and Calgary and for her kind heart. Petroula's insight, inspiration and kindness have been wonderful and are highly appreciated. I would like also to express my appreciation to the kind librarian Leslie Parker for her assistance. Joseph Kimetu transferred willingly his experience and passion while training me and I am most grateful to him. The generosity of Dr. Hussein and Dr. Hill in making laboratory equipment and space available is acknowledged. I benefitted from the knowledge of Dr. Bruce Jank and Rafaeal Gay-de-Montella in industrial and produced water treatment. I would like to express my sincere thanks to Abbas Zaidi for his mentorship and for imparting his knowledge to me. I also want to express my thanks to my great friends Zain, Sean, Hashem, Sobhan Fakhr Hossieni, Mostafa, Ebi, Mohammad, and Hossien for their inspiration and kind help.

The financial support of the Natural Sciences and Engineering Research Council of Canada (NSERC), Institute for Sustainable Energy, Environment and Economy (ISEEE), Centre for Environmental Engineering Research and Education (CEERE), and the Department of Chemical and Petroleum Engineering are gratefully acknowledged.

Dedication

To my mom, Talieh, who is an infinite source of love;

To my wonderful brothers Foad and Pedram;

And to my life teacher Dr. Azad.

Table of Contents

Abstract ii
Acknowledgements iv
Table of Contents vi
List of Tables viii
List of Figures and Illustrations ix
List of Symbols, Abbreviations and Nomenclature xi

CHAPTER ONE: INTRODUCTION 1
1.1 Background 1
1.2 Objectives 4
1.3 The Organization of This Thesis 5

CHAPTER TWO: LITERATURE REVIEW 6
2.1 Oil Sands Deposits and Operations 6
2.2 Oil Sands Naphthenic Acids 8
2.3 Toxicity and Corrosivity of Naphthenic Acids 11
2.4 Removal Methods 12
2.4.1 Chemical Oxidation 13
2.4.2 Membrane Removal 14
2.4.3 Bioremediation 14
2.4.4 Adsorption in NA Removal 14
2.5 Adsorption 15
2.6 Isotherms 16
2.6.1 Langmuir Isotherm 17
2.6.2 Freundlich Isotherm 17
2.6.3 Sips Isotherm (Langmuir-Freundlich) 18
2.7 Adsorbents 19
2.8 Chemical Activation for Production of Activated Carbon 22
2.9 Physical Activation 27
2.9.1 Biochar Production 28
2.9.2 Activation Stage 30
2.10 Objectives and Research 36

CHAPTER THREE: EXPERIMENTAL EQUIPMENT AND PROCEDURE AND THEORY 37
3.1 Raw Material Biomass 37
3.2 Biochar Production Method 38
3.2.1 Physically Activated Carbon Production 41
3.3 Chemically Activated Carbon Production 42
3.3.1 Yield 43
3.3.2 Burn-Off 43
3.4 Micrometric Tristar 44
3.4.1 Outgassing 45
3.4.2 Surface Area Measurement 46
3.4.3 Micropore Surface Area and Micropore Pore Volume 48

3.4.4 Pore Size Distribution....49
3.4.5 Total Pore Volume....49
3.4.6 Average Pore Size....49
3.5 Thermal Gravimetric Analysis....50
3.6 Adsorption Tests....51
3.6.1 Total Carbon Measurement....51
3.6.2 Inorganic Carbon Measurement....52
3.6.3 Batch Adsorption....52

CHAPTER FOUR: RESULTS AND DISCUSSION....54
4.1 Biochar production results....54
4.2 Physical and Chemical Activation....58
4.2.1 Burn-off and BET Surface Area versus Activation Temperature....58
4.3 Elemental analysis, C, H, N and S....70
4.4 TGA Results....72
4.5 Synthetic Adsorption Tests....75
4.6 Isotherm Data and Modeling....80

CHAPTER FIVE: CONCLUSIONS AND RECOMMENDATIONS....86
5.1 Conclusions....86
5.2 Recommendations....88

REFERENCES....90

List of Tables

Table 2.1 Composition of 4 different tailings ponds 9

Table 3.1 Proximate and ultimate analysis of biomass 38

Table 3.2 Produced activated carbon's conditions 40

Table 3.3 Temperature versus time for producing activated carbon 43

Table 4.1 Produced biochars and their yield 55

Table 4.2 Carbon content of produced biochar 57

Table 4.3 Produced activated carbon and their features 60

Table 4.4 BET surface area and microporsity of activated carbons 64

Table 4.5 Elemental analysis of produced activated carbon 71

Table 4.6 Adsorption results for activated carbon for initial point 18 mg/l 77

Table 4.7 Adsorption results for activated carbon for initial point 25.75 mg/l 77

Table 4.8 Adsorption results for activated carbon for initial point 32 mg/l 77

Table 4.9 Adsorption results for activated carbon for initial point 34 mg/l 78

Table 4.10 Adsorption results for activated carbon for initial point 42 mg/l 78

Table 4.11 Biochar sample TOC level in deionized water in the adsorption condition 79

Table 4.12 Modelling data for produced activated carbon 85

List of Figures and Illustrations

Figure 1.1 Biomass by product to activated carbon schematic process 3

Figure 2.1 Alberta's oil sands deposits, obtained from Alberta Geological Survey 6

Figure 2.2 Naphthenic acid structure 11

Figure 3.1 Temperature versus time for carbonization step 39

Figure 3.2 Carbonization and activation setup 41

Figure 3.3 Temperature versus time for producing activated carbon 42

Figure 4.1 Burn-off of AC series versus activation temperature 61

Figure 4.2 Surface area of AC series versus activation temperature 62

Figure 4.3 Surface area of N and M series versus activation temperature 62

Figure 4.4 Pore volume versus pore width for N1 66

Figure 4.5 Pore volume versus pore width for N2 66

Figure 4.6 Pore volume versus pore width for M1 67

Figure 4.7 Pore volume versus pore width for M2 67

Figure 4.8 Pore volume versus pore width for AC3 68

Figure 4.9 Pore volume versus pore width for AC4 68

Figure 4.10 Pore volume versus pore width for CA 69

Figure 4.11 Pore volume versus pore width for Com 69

Figure 4.12 Carbon content of activated carbon versus their activation temperature 72

Figure 4.13 Weight loss of N1 versus Time 73

Figure 4.14 Weight loss of N1 versus Temperature 74

Figure 4.15 Weight loss of N2 versus Time 74

Figure 4.16 Weight loss of N2 versus Temperature 75

Figure 4.17 Uptake ability versus initial concentration for different activated carbons 80

Figure 4.18 Isotherm data for N1 81

Figure 4.19 Isotherm data for N2 81
Figure 4.20 Isotherm data for M1 82
Figure 4.21 Isotherm data for M2 82
Figure 4.22 Isotherm data for CA 83
Figure 4.23 Isotherm data for Com 83

List of Symbols, Abbreviations and Nomenclature

Symbol	Definition
AC	Activated Carbon with Particle Size of <590 µm
a_m	The Molecular Projected Area
B	Constant for Langmuir Isotherm for BET Equation
B1000	Biochar with Particle Size of 590-1000 µm
B1400	Biochar with Particle Size of 1000-1400 µm
B590	Biochar with Particle Size of <590 µm
BET	Brunauer, Emmett, and Teller method
BOD	Biochemical Oxygen Demands
Boe	Barrel of Oil Equivalent
BTEX	Benzene, Toluene, Ethylbenzene and Xylenes
C_0	Initial Concentration
C_e	Equilibrium Concentration
E_1	Heat of Adsorption for the First Layer
E_L	Heat of Adsorption for the Second and Higher Layers
FC	Fixed Carbon Content
FTIR	Fourier Transform Infrared Spectroscopy
IC	Total Inorganic Carbon
M	Activated Carbon with Particle Size of 1000-1400 µm
N	Activated Carbon with Particle Size of 590-1000 µm
NA	Naphthenic Acids
P	Equilibrium Pressure
P_0	Saturation Pressure
PAH	Polycyclic aromatic hydrocarbons
Q	Uptake [mg of NA /g]
q_m	Langmuir Adsorption Constant for Aqueous Phase
R	Universal Gas Constant
Rpm	Round Per Minute
T	Temperature
TAN	Total Acid Number
TC	Total Organics
TGA	Thermal gravimetric analysis
TOC	Total Organic Carbon
V	Volume
V_M	Volume of the Adsorbed Chemical Required for Monolayer
V_{total}	Volume of All Pores
W	Weight of Adsorbent

Chapter One: **Introduction**

1.1 Background

Canada has the one of the largest oil deposits in the world located in northern Alberta and it is estimated to house nearly 15% of the world's crude oil supply. The in-situ recovery technology for the Athabasca, Cold Lake and Peace River oil sands have given Canada what are currently recognized as the third largest oil reserves in the World. The majority of these reserves are in the form of heavy oil and bitumen. The oil sands are typically composed of 11% bitumen, 5% water, and 84% sand and clay by weight (Alberta Environment, 2012).

There are two general methods for extraction of oil sands: in-situ thermal recovery and surface mining. The in-situ thermal recovery methods use steam injection to heat the reservoir and decrease the bitumen viscosity allowing it flow and be pumped to the surface. The less deeply buried oil sands are mined with specialized machinery including large shovels and trucks to move the whole oil sand to the processing plants. In surface mining, oil sands are excavated from a shallow pit to a processing unit, which is basically a flotation unit, and mixed with hot caustic water to extract the bitumen. In both in-situ thermal and mining operations, water is a critical material needed for the extraction process.

About 12 volumes of water are needed to produce one volume of bitumen in oil sands surface mining operations, with some of this water ending up in tailings ponds (Allen, 2008a). Because the majority of the water is recycled and reused in the processing, the mining operations need 2 to 4 volumes of make-up water for each volume of bitumen produced. The in-situ recovery operations use about 0.5 volumes net of water for each volume of bitumen produced since these operations are required to recycle over 90 percent of the produced water. Based on Alberta's zero-discharge law, producers cannot return the water to the rivers, as the water in tailings ponds contains caustic and is contaminated by soluble organic compounds. The organics

in the water are mainly polycyclic aromatic hydrocarbons (PAHs), benzene, toluene, ethylbenzene and xylenes (BTEXs) and naphthenic acids (NAs) (Allen, 2008a). These organic contaminants are found in the produced water due to the contact of high temperature water and steam with bitumen. NAs are the major organic contaminants found in oil sands surface mining wastewater and occur in high concentrations, up to 120 mg/l, in tailings ponds. The effects of NAs on mammals and the environment have been investigated in many studies (Gamal El-Din et al., 2012, Rogers et al., 2002, Clemente and Fedorak, 2005). NAs also cause problems in the boiler feed water treatment systems and the boilers due to their corrosive nature and their tendency to form scale deposits (Perrich, 1987). Another benefit of removal of organics including NA is to reduce the greenhouse gas emission from tailing ponds. Due to the anaerobic consumption of the NA by microorganisms, tailing ponds emit large amounts of methane, a potent greenhouse gas with about 23 times the global warming potential of CO_2 (Siddique et al., 2008). Therefore removal of organics from tailing ponds can decrease the greenhouse gas emission problem.

Several methods have been proposed for the removal of NAs: catalytic reaction, bioreactor, membrane technology and adsorption. The latter method is deemed to be one of the more promising solutions for NA removal. Activated carbon (AC) has shown excellent performance in the adsorption of organics, but it may be expensive to produce depending on the raw material used and the production method employed. Changing the raw material may decrease the price of AC; and, many researchers have substituted cheap raw material, such as municipal waste, tires and agricultural waste for the production of AC (Ng et al., 2003, Choy et al., 2005). Depending on how it is produced, the carbon footprint of biochar and the activated

carbon produced from it may be negative and can be considered as a carbon sink or a low carbon source of energy.

The production of AC is generally divided in two processes: physical activation and chemical activation. In chemical activation, raw material is impregnated with a chemical, such as potassium hydroxide or phosphoric acid, and then placed in a reactor for pyrolysis (Yang, 2003). The disadvantages of chemical activation are the consumption of expensive and hazardous chemicals and the washing step required after production.

Physical activation is basically a two-stage process. In the first stage, raw material is pyrolyzed in an inert atmosphere to drive off volatile components leaving a richer carbonaceous material, called biochar. In the second stage, the produced biochar is activated at a higher temperature using an activation gas, such as carbon dioxide or steam (Yang, 2003). Higher energy consumption and lower yields are disadvantages of physical activation over chemical activation. Physical activation is an older process than chemical activation, and many current AC production facilities are using physical activation as shown in Figure 1.1.

Figure 1.1 Biomass by product to activated carbon schematic process

The produced AC's properties, such as final yield, surface area and adsorption capacity, are dependent on the raw material and production process (Aroua et al., 2008). Therefore, a clear understanding of the effects of the activation process and raw material on the produced AC are crucial for the proposal of a new process.

1.2 Objectives

The main goal of this research is the development of a process that converts biomass to AC, which can then remove naphthenic acids (NAs) from tailings pond water or in-situ recovery process produced water. The specific objectives of this project are:

1. To develop a process to obtain AC from biomass using carbon dioxide (CO_2) and phosphoric acid (H_3PO_4).
2. To investigate the effects of the activation temperature and the particle size of the raw material on the surface area and yield of the produced AC.
3. To determine the NA adsorption capacity of the produced ACs using a commercially available mixture of NA and deionized water to model tailings pond water.
4. To recommend the optimal activation conditions, based on the reactor used in experiments, for producing an effective AC adsorbent for NA removal from tailings pond water.
5. To obtain the adsorption isotherm of NA for each AC.

1.3 The Organization of This Thesis

This thesis contains five chapters, in addition to a table of contents, a list of tables, a list of figures and two appendices.

Chapter Two is an overview of AC production from carbonaceous raw material, the methods of AC production, the issue of NAs in Alberta oil sands tailings ponds, the physical and chemical characterization techniques used for AC, and the applications of ACs in the oil and gas industry.

Chapter 3 describes the experimental methods for AC production, the characterization techniques used on the used biomass and the produced ACs, and NA adsorption.

Chapter 4 discusses the results obtained from the experiments. The effects of different operating parameters on product distribution and quality are presented.

Finally, Chapter 5 presents the conclusions and recommendations for future study.

Chapter Two: **Literature Review**

2.1 Oil Sands Deposits and Operations

Alberta has some of the largest oil reservoirs in the World. According to a government report, Alberta's three major oil sands areas, Athabasca, Peace River and Cold Lake, contain approximately 1.7 trillion barrels of bitumen in place and proven measures indicate there are currently 173 billion barrels of recoverable oil (Alberta Environment, 2011). The locations of these deposits are shown in Figure 2.1 (Alberta Environment, 2012). The largest of these deposits is the Athabasca oil sands. Alberta's boreal forest covers an area of 381,000 square kilometres (147,100 square miles) (Alberta Environment, 2010), and it has been estimated that the oil sands deposits underlie an area of approximately 142,000 square kilometres or 700 million m^2 (Allen, 2008a). Based on data from the National Energy Board, oil production from the oil sands has reached 1 million barrels per day and is projected to triple over the next decade.

Figure 2.1 Alberta's oil sands deposits, obtained from Alberta Geological Survey (2012)

The Government of Alberta defines oil sands as "sand, clay or other minerals saturated with bitumen". Oil sands are also defined in the Mines and Minerals Act as "(i) sands and other rock materials containing crude bitumen, (ii) the crude bitumen contained in those sands and other rock materials, and (iii) any other mineral substance (except natural gas) associated with the above-mentioned crude bitumen, sands or rock materials and includes a hydrocarbon substance declared to be oil sands under section 7(2) of the Oil Sands Conservation Act." (Alberta Environment, 2011).

Generally there are two methods for the extraction of bitumen in Alberta, surface mining and the in-situ extraction using thermal recovery methods. In the thermal method, processes such as Steam Assisted Gravity Drainage (SAGD) or Cyclic Steam Stimulation (CSS) use steam for heating the reservoir and decreasing the viscosity of bitumen. During these processes, the steam-to-oil ratio (SOR) is usually greater than 3 where steam volume is measured as cold water equivalent. With approximately 90 percent of the produced water recycled for steam generation, the make-up water required for in-situ recovery is about 0.5 volumes per volume of bitumen produced. In the hot water extraction process used to separate bitumen from mined oil sand 12 to 14 volumes per volume of water are required but with the high amount of water recycling used, the make-up water requirement is 2 to 4 volumes per volume. Nevertheless, a large amount of water is required for both mining and in-situ extraction process and significant volumes of water are being treated to allow high percentages to be recycled (Deriszadeh, 2009). The in-situ thermal methods are employed when the oil sand reservoirs are buried to depths greater than 150 metres and the majority of the Athabasca deposit is found below this depth. Surface mining operations are currently able to economically extract oil sands buried to depths up to 75 metres representing only about 20 percent of the resource (Allen, 2008a). According to Government of

Alberta statistics, in-situ thermal methods will be required for the remaining 80% of the Athabasca deposit (Alberta Environment, 2012). Both Cold Lake and Peace River deposits also require development through in-situ recovery methods.

The method for the extraction of bitumen from the oil sands in surface mining is a unique mining method, called the Clark hot water process. Basically this method utilizes flotation and mechanical separation. Caustic soda (NaOH) is added to enhance the release of surfactants and improve bitumen separation. Water plays an important role in this process and given the large scale of the current and planned projects, there is concern about the water supply for future production (Allen, 2008a).

Oil sands mines consume large volumes of water, importing an average of 3 barrels of river water for every barrel of oil produced (Allen, 2008a). Following contact with bitumen at high temperature, the processed water is too toxic for the environment, due to its alkalinity, salinity and organic content resulting from the leaching of organics in the bitumen (MacKinnon, 1993). The oil sands industry is facing new challenges regarding the use of water due to protection of local freshwater resources, such as the Athabasca River Basin (Allen, 2008a). Due to Alberta's zero discharge regulation, oil sands producers cannot return the processed water back to the rivers and, therefore, must store all processed waters and tailings onsite, resulting in large volumes of water stored in tailings ponds. The current volume of tailings pond water is estimated to exceed 700 million m^3 (Barnard, 2011, Allen, 2008a).

2.2 Oil Sands Naphthenic Acids

Generally the processed water accumulated in tailings ponds is saline, contains suspended solids, oil and grease, and is polluted with a range of organic substances, such as polycyclic aromatic hydrocarbons (PAHs) and naphthenic acids (Small, 2011). With the recycling of

tailings pond water for use in further extraction processes, the concentrations of these pollutants increase dramatically over time (Gamal El-Din et al., 2011).

Allen (2008a) reviewed the literature for a better understanding of the water situation in Alberta. For a clear idea concerning the composition of tailings ponds, four different water analyses were provided and are shown in Table 2.1 (Allen, 2008a). In Table 2.1, the concentrations of the naphthenic acids (NAs) are in the range of 40 to 70 mg/l. Organic materials in the processed waters, which are considered to be major contaminants and sources of toxicity, may be in the form of organic acids, aromatic compounds and bitumen (Allen, 2008a), (Withby, 2010). Naphthenic acid is considered to be the main organic pollutant in the tailing ponds, with 80% of the organic acid fraction being comprised of oil sands naphthenic acids, a term referring collectively to all of the carboxylic acids founds within crude oil (Allen, 2008a). The term 'naphthenic acid' was initiated with the first observation of the acidity in naphthenic-based crude from the Baku Region in 1920's (Zhang, 2005).

Table 2.1 Composition of 3 different tailings pond waters (Allen 2008a).

Variable (mg/l)	Syncrude MLSB (1985-1998)	Syncrude Demonstration Ponds (1996-97)	Suncor Tailings Ponds (1982-1998)	Athabasca River 2001	Regional Lake
Dissolved organic carbon	58	26-58	62-67	7	14-27
Biochemical oxygen demand	25	-	<10-70	<2	-
Chemical oxygen demand	350	-	86-525	40	-
Oil and grease	25	-	9-31	<.5	-
Naphthenic acid	49	3-59	68	<1	1-2
Phenols	0.0008	.001-.003	.03-1.8	<.001	.002-.004
Cyanide	0.5	-	.01-.04	.004	-
Polycyclic aromatic hydrocarbon	.01	-	-	-	-
Toluene	-	-	1-3	-	-
Benzene	-	-	<0.6-6	-	-
Benzene toluene ethylbenzene xylene	<.01	-	--	-	-

In the Kirk-Othmer Encyclopedia of Chemical Technology, naphthenic acids (NAs) are defined as "monobasic carboxylic acids of the general formula RCOOH, where R represents the naphthenemoiety consisting of cyclopentane and cyclohexane derivatives" (Brient and Doyle 2000). Brient and Doyle (2000) also consider that NAs are composed predominantly of alkyl-substituted cycloaliphatic carboxylic acids, with smaller amounts of acyclic aliphatic (paraffinic or fatty) acids. Aromatic, olefinic, hydroxy and dibasic acids are regarded as minor components.

NAs can be shown by the general formula $C_nH_{2n-z}O_2$. Brient and Doyle (2000) proposed that z is equal to 0 for saturated, acyclic acids and increases to 2 in monocyclic NAs, 4 in bicyclic NAs, 6 in tricyclic acids, and 8 in tetracyclic acids. NAs in the range of C-7 to C-12 consist mainly of monocyclic acids. The more complex acids contain larger proportions of multi-cyclic condensed compounds. Figure 2.2 shows the common structures for the homologues of NA (Brient and Doyle, 2000).

Another feature of NA that is important in the separation of organics is the acidity behaviour and hydrophobic nature of the material. The Kirk-Othmer Encyclopedia of Chemical Engineering states that NA behave as typical carboxylic acids with similar acid strengths, as the higher fatty acids and dissociation constants are in the order of 10^{-5} to 10^{-6} (Brient and Doyle, 2000). Therefore, NA are considered to be weaker than lightweight carboxylic acids, such as acetic, yet stronger acids than phenol and cresylic acids. As a result of weak acidic behaviour of NA, their solubility is highly dependent on pH: as the pH increases, so does solubility. Small (2011) stated that pH levels above neutral also increase the mobility of NA in tailing ponds and allow for higher uptake by plants and animals.

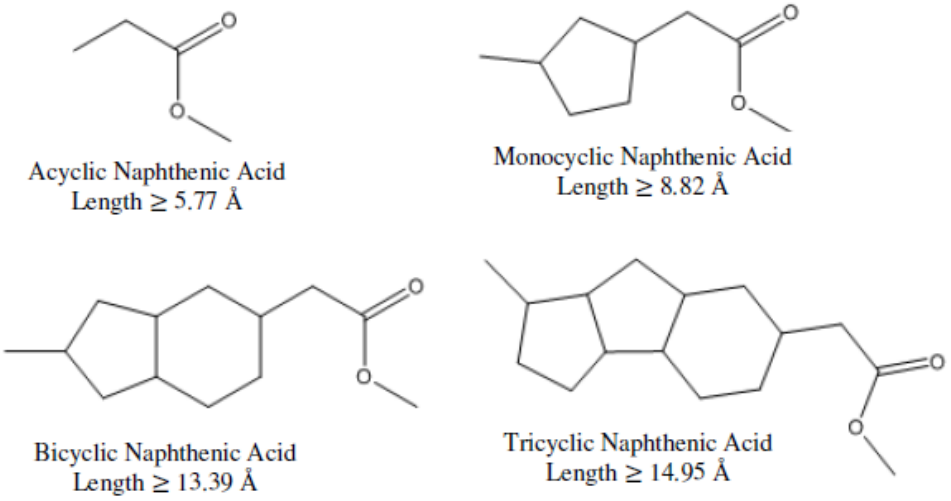

Figure 2.2 Naphthenic acid structure, (Small, 2011)

2.3 Toxicity and Corrosivity of Naphthenic Acids

Several studies have been conducted to examine the toxicity of NAs on humans, animals and their environments. Certain NA levels have been known to demonstrate changes, both physical and pathological, in Wistar rats, which have been used as a model of mammals (Rogers et al., 2002). These authors have concluded that NA concentrations greater than 2.5–5 mg/L in refinery effluent would be toxic to surrounding fish and wildlife (Rogers et al., 2002)

Clemente and Fedorak (2005) did a comprehensive study of tailings pond toxicity, determining that tailings pond water contains 20–120 mg/L of NAs. Oil sands companies operate under a zero liquid discharge policy; thus, none of these waters can be intentionally released back into the environment, and much of the water is recycled through the extraction process. However, when the oil sands operations cease, all the disturbed land and the water in tailings ponds must be reclaimed, and the NA concentrations reduced to below toxic levels (Clemente and Fedorak, 2005).

In Withby's study (2010), oil sands NA were shown to be acutely and chronically toxic to a variety of organisms, including fish, amphibians, zooplankton, mammals (rats and guinea pigs), as well as bacteria.

There are also several studies that address NA corrosivity. Clemente and Fedorak (2005) stated that oil sands NAs are corrosive to the oil processing and refining infrastructure. Corrosion occurs through the formation of hydrogen gas at typical operating temperatures (200 to 400°C), causing chelation of metal ions in the presence of carboxylic acid groups. The corrosion rate and amount is directly related to the following parameters: temperature, availability of carboxylic acid groups, molecular composition of the present metal compounds and increasing alkyl chain length (Clemente and Fedorak, 2005).

2.4 Removal Methods

Removal of NA compounds from crude oils is regarded as one of the most important processes in heavy oil upgrading. NA removal efficiency is characterized by the total acid number (TAN) measurement (Zhang et al., 2005), which is defined as the milligrams of potassium hydroxide (KOH) required for neutralizing the acidity of one gram of oil. Current industrial methods for removing NA from heavy crude oil either depend on dilution or caustic washing methods to reduce the TAN (Lehr, 2005). However, neither of these methods is considered to be consistently reliable. According to Zhang et al. (2005), this is due to the blending of a high TAN crude oil with a low TAN oil, which may reduce the NA content to an acceptable level, but the acidic compounds remain and the value of the low TAN oil is diminished. They also expressed that caustic treatment can remove NA, but the process generates significant amounts of wastewater and emulsions that are problematic to treat (Zhang et al., 2005).

NA removal methods can generally be categorized in 4 main groups: (i) chemical oxidation, (ii) membrane removal, (iii) bioremediation, and (iv) adsorption (Allen, 2008b). Allen (2008b) also mentioned groups of methods as possible solutions for de-oiling in Alberta oil sands surface mining wastewater treatment. Each of these technologies is reviewed in the following subsections.

2.4.1 Chemical Oxidation

Catalytic decarboxylation is considered to be one of most established methods in organic and biochemical processes. Catalytic decarboxylation can also be used to identify the structure of materials. Copper based catalysts are one of most well-known catalysts developed for this reaction. Zeolite has also been applied in the catalytic decarboxylation of benzoic acid, but the reaction occurred at around 400 °C (Zhang et al., 2006). Unfortunately, most studies are limited to the laboratory scale, not yet at field scale; therefore, their feasibility for industry application is unknown (Allen, 2008b).

In 2006, catalytic decarboxylation of carboxylic acid model compounds and NA removal from crude oil were investigated. A metal oxide catalyst, magnesium oxide (MgO), has been developed; and, its effectiveness in catalyzing decarboxylation reactions involving carboxylic acid compounds, such as NA, has been determined based on the formation of CO_2 and the conversion of the acid (Zhang et al., 2006).

The hydroxyl radical mechanism in the initiation of the degradation of a typical oil sands process water alicyclic carboxylic acid was studied using cyclohexanoic acid (CHA) as a model compound by Drzewicz et al. (2010). They used vacuum ultraviolet irradiation (VUV, 172 nm) and ultraviolet (UV, 254 nm) irradiation in the presence of hydrogen peroxide (H_2O_2). It was concluded that CHA undergoes degradation through a peroxyl radical. In both processes, the

decay of the peroxyl radical leads predominantly to the formation of 4-oxo-CHA with minor amounts of hydroxy-CHA (detected only in UV/H2O2) (Drzewicz et al., 2010).

2.4.2 Membrane Removal

Membrane technology is considered to be one of the potential technologies for wastewater treatment in the oil sands industry. Allen (2008b) showed decreased organic concentration in water with ultrafiltration, microfiltration, nanofiltration and reverse osmosis. The effectiveness of each of these technologies depends on their individual design. Fouling by organics and high cost of membranes are the main disadvantages of membrane methods.

2.4.3 Bioremediation

Another potential technology for oil and gas wastewater treatment is biological treatment. Biological treatment refers to the use of microbes to remove organic pollutants from wastewater in low rate processes, such as stabilization ponds and lagoons, and high rate suspended growth processes, such as activated sludge, trickling filters and rotating bioreactors. Activated sludge is widely used in the biological treatment of municipal wastewater, where it achieves high removal rates for biochemical oxygen demand (BOD) and chemical oxygen demand (COD) (Allen, 2008b). The feasibility of bioremediation for oil sand waste water is still unknown.

2.4.4 Adsorption in NA Removal

Adsorption is a promising removal method for organics. Allen (2008b) has mentioned that adsorption is a potential process for wastewater treatment for surface mining tailings ponds. The proposed adsorbents can be activated carbon (AC) or an ion-exchange resin. AC has always been an excellent adsorbent for organic materials, such as methylene blue ($C_{16}H_{18}N_3SCl$) and

phenol (Benadjemia et al., 2011, Perrich, 1981, Tan et al., 2008, Girods et al., 2009, Lua and Jia, 2009). The performance of AC in removing NA has been investigated by Barnard in 2011 and Small in 2011 who used delayed petroleum coke to produce AC.

Gamal El-Din et al. (2011) studied NA speciation and removal during petroleum-coke adsorption and ozonation of oil sands wastewater. This study examined, for the first time, the impacts of pretreatment steps, including filtration and petroleum-coke adsorption on ozonation requirements and performance. They also evaluated the effect of the initial tailings pond pH on treatment performance and the effect of ozonation and its impact on tailings pond toxicity and biodegradability. The degradation of more than 76% of the total acid-extractable organics was achieved using a semi-batch ozonation system, utilizing an ozone dose of 150 mg/L. Petroleum-coke adsorption was found to be effective in reducing total acid-extractable organics by 91%, NA content by 84%, and oil sand processed water toxicity from 4.3 to 1.1 toxicity units (Gamal El-Din et al., 2011).

The problem of using petroleum-coke as a precursor is the leaching out of vanadium and other heavy metals in the water (Jia et al., 2002). Obviously, there are limitations on the amount of heavy metal allowed in the water due to health and operational maintenance concerns. Therefore petroleum-coke may not be an appropriate precursor of AC.

2.5 Adsorption

Adsorption is a fairly old technique. It is a separation method that can transform a mixture of substances into two or more products that differ from each other in composition. This process can occur physically or chemically (Bansal, 2005). After the creation of synthetic zeolites in 1959, innovations in absorbent development and adsorption process cycles have

played important roles in the chemical, petrochemical and pharmaceutical industries (Yang, 2003).

The most widespread sorbents currently are activated carbons (ACs), zeolite and silica gel. Among these, AC, which is considered to be a hydrophobic material, is used as an all-purpose sorbent. One of the first usages of AC as an absorbent was in England's sugar industry in 1794 to decolorize sugar syrup (Yang, 2003).

One of the main parameters considered in the adsorption process is the choice of the most appropriate and most efficient sorbents for a specific removal process. In the following section, studies on NA adsorption are reviewed.

2.6 Isotherms

The selection of a proper sorbent for a given separation is a complex problem. The predominant scientific basis for sorbent selection is the equilibrium isotherm. The diffusion rate is generally secondary in importance. Isotherm refers to the relationship between the amounts of adsorbate on the adsorbent at equilibrium, and isotherms are used to describe adsorption. By knowing the isotherm of adsorption, one can find the carrying capacity of the adsorbent, regeneration method, the length of the unusable bed and product purities. Therefore, determination of the equilibrium isotherm is important for designing the whole process.

In liquid adsorption, parameter q is defined below and is used to plot the isotherm:

$$\boldsymbol{q} = \frac{\boldsymbol{V}\times(\boldsymbol{C_0}-\boldsymbol{C_e})}{\boldsymbol{m}} = \left[\frac{\boldsymbol{g\ adsorbed}}{\boldsymbol{g\ of\ adsorbent}}\right] \qquad 2\text{-}1$$

where V is the volume of the adsorption chamber, C_0 is the initial concentration, Ce is the equilibrium concentration, and m is the mass of adsorbent. The isotherm is actually the mathematic relationship between the q and equilibrium concentration (Do, 1998).

There are several mathematical equations for determining the isotherm. Some of these equations have theoretical basis, such as Langmuir and Freundlich isotherms; and, some are based on empirical models, such as Sips and Toth (Do, 1998). In following subsections, these isotherms are briefly discussed.

2.6.1 Langmuir Isotherm

The Langmuir isotherm is the one of the oldest formulations, developed in 1918 based on kinetic theory. The basic concept is that the rate of bombardment of molecules onto the surface and the corresponding evaporation (desorption) of molecules from the surface are equal at equilibrium. Langmuir also assumed a homogeneous surface, where adsorption energy is even on the surface. Monolayer adsorption and fixed site are other important assumptions of the Langmuir theory, i.e. each site can adsorb only one molecule or atom at a time, and molecules are fixed in those sites. The Langmuir equation may be written

$$\boldsymbol{q = q_m \frac{BC_e}{1+BC_e}} \qquad 2\text{-}2$$

where q_m and B are constants of this equation and can be obtained by curve fitting of experimental data.

2.6.2 Freundlich Isotherm

The Freundlich equation was established in 1932. Freundlich's isotherm performs well for describing the adsorption of organics from aqueous streams onto AC. Many researchers consider this isotherm as an empirical equation (Do, 1998). The equation form is:

$$q = KC_e^{\frac{1}{n}} \qquad 2\text{-}3$$

where C_e is the equilibrium concentration of the adsorbed species, and K and n are constants.

Parameter n is usually greater than one; and, the greater n is, the more nonlinear is the isotherm. The nonlinearity can be interpreted as irreversibility. As the behaviour deviates further away from that of the linear isotherm, which is determined by the amount adsorbed versus pressure, the adsorption isotherm becomes more nonlinear. Therefore, it is generally valid in the narrow range of the adsorption data.

The parameters of the Freundlich equation can be found by plotting $\log_{10}$ (q) versus $\log_{10}(C_e)$

$$\log_{10} q = \log_{10} K + \frac{1}{n}\log_{10} C_e \qquad 2\text{-}4$$

which gives a straight line with a slope of (1/n) and an intercept of $\log_{10}(K)$ (Do 1998).

2.6.3 Sips Isotherm (Langmuir-Freundlich)

One of the problems of the Freundlich isotherm is the concentration of adsorbed material increasing with the amount adsorbed. However, in reality, there is a limit to the amount of adsorbed material. Therefore, Sips in 1948 modified the Freundlich isotherm with the Langmuir equation; and, established a limit in this modified equation. The Sips equation is presented in the following form:

$$q = q_m \frac{(bC_e)^{\frac{1}{n}}}{1+(bC_e)^{\frac{1}{n}}} \qquad 2\text{-}5$$

where q_m, b and n are constants.

The difference between the above equation and the Langmuir equation is the exponential factor. If n is equal to one (n = 1), the Sips equation reduces to the Langmuir equation. Do (1998) stated that n can be considered as characterizing the system heterogeneity. The isotherm equation

is sometimes also referred to as the Langmuir-Freundlich equation, as it is an amalgamation of both (Do, 1998).

2.7 Adsorbents

There are few studies regarding the removal of NA via non-AC adsorbents. One of these rare studies was conducted by Gaikar and Maiti, who researched the adsorption of NA on both commercially-used weak and strong anion-exchange resins. Their studies were focused on the removal NA from crude oil. They claimed that acidity of NA could be useful for the separation of NA from crude oil. They also stated that liquid-liquid extraction using alcoholic alkali or ammonia solutions is one of the more effective methods for recovering NA. A 94% removal from crude oil was claimed, with a similar purity of the recovered NA salt, but these systems are liable to form stable emulsions (Gaikar and Maiti, 1996).

For solutions containing a solute at a low concentration, it is better to use adsorptive techniques for separation. The adsorption on ion-exchange resins would strongly depend on the functional group on the polymeric backbone of the resin (Gaikar and Maiti, 1996). Therefore, some adsorption experiments on weak and strong commercial anion-exchange resins were performed. Zeolites, bentonite and polyvinyl pyridine were used as adsorbents; and, as for detecting NA, they used titration with alcoholic KOH to determine the acid value. They concluded that the zeolite capacity was low due to the comparable sizes of the pores and molecules and that the major interactions existing between tertiary amine groups on the ion-exchange resins and NA were acid based. They also showed that the adsorption was governed by the internal diffusional resistance and was also characterized by its dependence on concentration. The capacity of Na-X zeolite was minute in comparison to those of other adsorbents (Gaikar and Maiti, 1996).

Activated carbon is the most widely used sorbent. Its manufacture and use dates back to the 19th century. Its usefulness is mainly derived from its large micropore and mesopore volumes and the resulting high surface area (Yang, 2003). The manufacturing processes of AC are basically comprised of the following steps: raw material preparation, low-temperature carbonization, and activation. Wood, peat, coals, petroleum coke, bones, coconut shells and fruit nuts have been used as raw material for producing AC. Raw material process conditions have significant effects on the final features of the produced AC (Yang, 2003).

Activated carbon is a promising adsorbent for removal of organics, due to its affinity for organic materials. There are several studies regarding the adsorption of volatile organic compounds from the gas phase using AC (Perrich, 1981).

Activated carbon plays an important role in wastewater applications. Different studies have shown that mesoporosity (near or larger than 30 Å) is desirable for liquid-phase applications, where micropore sizes (10 to 25 Å) are more suitable for gas-phase applications (Yang, 2003) (Perrich, 1981). Activated carbon is used in municipal water treatment as a polishing step to remove all undesirable organics in the water. Activated carbon is generally used in granular form (GAC) or packed shape (PAC). One of the main applications of AC is adsorbing phenol and methylene blue in the aqueous phase (Perrich, 1981).

The widespread use of AC has, however, been restricted due to its high cost. Thus, many researchers are looking for a low-cost alternative precursor, such as agricultural by-products, waste tires, sewage sludge and agricultural manures, for the production of AC. There are a variety of raw materials that can be used for the production of AC: corn, rice husks, nutshells, peat, wood, coconut husk fibres, lignite, coal and petroleum pitch (Bagheri and Abedi, 2009, Stavropoulos and Zabaniotou, 2009, Yalçın and Sevinç, 2000, Sricharoenchaikul et al., 2007).

Using biomass based AC or biochar as adsorbent can also decrease the CO_2 footprint. It can be used as a carbon sink. In the study that was done by Lehmann and Joseph (2009), it was shown that physically activated carbon can play a role in carbon sequestration and therefore act as a carbon sink. In the other words, AC from biomass can have a net negative carbon footprint.

Although the process for manufacturing AC has been largely empirical, there is now a considerable understanding of the fundamental processes. With the careful choice of the precursor and careful control of production conditions, it is possible to tailor the pore structure of the final produced AC for a specific application (Perrich, 1981).

The production of AC involves the pyrolysis of the raw carbonaceous material in an inert gas environment to produce a richer carbon material and the process usually takes place in two phases: carbonization and activation (Bansal, 2005). Carbonization involves the distillation of volatile compounds (such as oxygen, hydrogen, nitrogen and sulphur species) from the raw materials. Carbonaceous raw materials have a close structure to graphite: flat layers of aromatic structures are cross-linked in an ordered fashion. In addition, during carbonization, the carbon atoms that are left in the raw material restructure themselves in a disordered cross-linked manner (Bansal, 2005). During the activation phase, these compounds that plug up the interstices are removed. The remaining material then has a random pore distribution of various shapes and widths, which is now called an AC (Bansal, 2005).

After carbonization, the resulting biochar needs to be activated in order to enlarge the rudimentary pores created during carbonization and increase surface area and therefore adsorption capacity. The activation process can be done in two ways: (i) physical activation, and (ii) chemical activation. Physical activation is the development of porosity by gasification with an oxidizing agent at relatively high temperatures. Chemical activation involves treating of the

precursor with a chemical agent prior to activation and is the other important industrial process for the production of AC. The most common chemical activating agents are KOH, phosphoric acid and zinc chloride. In comparison to physical activation, the chemical activation mechanism is not well understood (Hayashi et al., 2000).

In physical activation of biomass, the first step is carbonization at 400–500°C to remove the volatile components in the biomass and then partial gasification at 800–1000°C to develop the porosity and surface area. The intrinsic surface reaction rate is much slower than the pore diffusion rate, so activation agents, such as carbon dioxide and steam, are used in the activation stage, thereby ensuring the uniform formation of pores throughout the solid pellets (Yang, 2003).

In chemical activation, the raw material is impregnated with a chemical material, such as a strong base, strong acid or salt (Guo and Lua, 2003a, Yang, 2003, Yang and Lua, 2006, Azargohar and Dalai, 2008, Daud et al., 2000, Jia and Lua, 2008, Lua and Jia, 2009). The second step is the activation of the impregnated raw material at temperatures between 500 to 900 °C. The produced AC then needs to be washed to remove any excess activation chemical. It has been stated that, without washing, ACs have a reduced surface area. Washing is done until a pH of 7 is reached (Barnard, 2011). Chemically activated carbons generally show a higher surface area than those of physically activated carbons (Yang, 2003).

2.8 Chemical Activation for Production of Activated Carbon

In the chemical activation process, the precursors are impregnated with activation chemicals, such as phosphoric acid, zinc chloride, potassium carbonate, sodium hydroxide or potassium hydroxide and carbonized at desired conditions in a single step. In many studies, chemically activated carbon is favoured, due to moderate activation temperatures, single-step activation, higher yields and better porous structure. The washing step, which is used to

completely remove the activation agent from the AC, and expensive chemicals are disadvantages of chemical activation (Lim et al., 2010, Toles et al., 1997).

The mechanism of chemical activation is basically the dehydration of raw materials to prevent production of tar, thereby decreasing the rate of the formation of other volatile products. Phosphoric acid and zinc chloride are used for the activation of lignocellulosic materials that have not been carbonized previously; whereas metal bases, such as KOH, are commonly used for the activation of coal precursors or chars (Lim et al., 2010, Salehi et al., 2011).

The effect of phosphoric acid in the production of AC has been studied by several researchers. Lim et al. (2010) produced a bamboo-based AC, prepared with a microwave-induced activation process using phosphoric acid as the activating agent. The effects of various factors, such as microwave power, radiation time and phosphoric acid / carbon ratio, on the activation were studied. They reached the conclusion that the surface area of 1432 m^2/g and a carbon yield of 48% could be reached with the optimal conditions. By increasing the phosphoric acid / carbon ratio, there was enhanced development of the pore structure.

Benadjemia et al. in 2011 used phosphoric acid to produce AC, which was prepared by the pyrolysis of artichoke leaves impregnated with phosphoric acid at 500°C for different impregnation ratios: 100, 200 and 300 wt.%. The impregnation ratio was found to govern the porous structure of the prepared ACs. Low impregnation ratios (~100 wt.%) led to essentially microporous and acidic ACs, whereas high impregnation ratios gave essentially microporous–mesoporous carbons with specific surface areas as high as 2038 m^2/g (Benadjemia et al., 2011).

The impregnation ratio was studied by Laine et al. in 1989. Activated carbon was prepared from coconut shells impregnated with phosphoric acid using a one-step carbonization

procedure. Higher surface areas and mesoporosity resulted with increased acid concentrations of the impregnating solution (Laine et al., 1989).

Girgis and El-Hendawy (2002) used date pits as a precursor for the production of porous carbons in a chemical scheme using phosphoric acid. The raw materials were impregnated with different concentrations of phosphoric acid (30–70 vol. %), followed by pyrolysis at 300, 500 or 700°C. The textural characteristics of the products were determined by adsorption of nitrogen (N_2) at -200°C K, as well as iodine, phenol and methylene blue values. The carbons obtained at 300°C had low porosity, although with an anomalously high capacity for the uptake of targeted molecules from solutions. It was suggested that the phosphoric acid caused physical and chemical modifications on the botanical structure by penetration, particle swelling, partial dissolution of the biomass, bond cleavage and reformation of new polymeric structures resistant to thermal decomposition. In addition, raw date pits were proposed to be composed of low-porosity and compact cellular structures that need higher acid concentrations and/or temperatures to attain the optimal effect, normally reached at lower temperatures in cases of other feedstocks of botanical origin.

Lim et al. (2010) found that ACs derived from palm shells with good textural characteristics (Brunauer–Emmett–Teller (BET) surface area > 1000m^2/g) had yields lower than 30%, irrespective of the activation process. Given the ability of chemical activation methods to produce high yielding ACs, the study utilized a two-stage activation process in a self-generated atmosphere to prepare the ACs. The yield of AC was found to be around 50%, while the BET surface area of the activated material, corresponding to an iodine number of 1035 mg/g, was estimated to be 1109 m^2/g, with a pore volume of 0.903 cm^3/g and an average pore diameter of 3.2 nm (Lim et al., 2010).

Aravindhan et al. (2009) prepared AC from two types of macro-algal biomass, Sargassum longifolium and Hypnea valentiae, which were examined for the removal of phenol from aqueous solutions. The ACs were produced by zinc chloride activation. Experiments were carried out at different activating agent / precursor ratios and carbonization temperatures, which had significant effects on the pore structure of the carbon. The produced ACs were characterized by BET surface area (SBET) analysis and iodine number. Carbons ZSLC-800 and ZHVC-800 showed a surface area around 802 and 783 m^2/g , respectively.

Adinata et al. (2007) used palm shells to prepare AC using potassium carbonate as the activating agent. The influence of the carbonization temperatures (600–1000°C) and impregnation ratios (0.5–2.0 weight of chemical/ weight of precursor) of the prepared AC on the pore development and yield were investigated. Results showed that, in all cases, the yield decreased with increasing carbonization temperature and impregnation ratio, while the adsorption of CO_2 increased progressively. The specific surface area of the ACs was at a maximum at about 1170 m2/g at 800°C for an activation duration of 2 hours and at an impregnation ratio of 1.0.

Guo and Lua (2003a), detected surface functional groups on oil palm shell (a biomass by-product from palm oil mills) adsorbents prepared by phosphoric acid and KOH activation using Fourier transform infrared (FTIR) spectroscopy. The effects of the activation temperature and chemical/sample ratio on the characteristics of the AC were investigated. The resulting AC had a relatively high yield. Moreover, potassium ions accelerated the reaction as catalysts during gasification of chars by CO_2. For chars with mid-impregnation, KOH acted in two ways: (i) formation of metallic potassium by dehydration and (ii) conversion into potassium carbonate. Large BET surface areas indicated well-developed pore structures for all impregnation

treatments used in this study, and the predominant microporosity of the prepared ACs can lead to their application in gas-phase adsorption.

Guo and Lua (2003b) produced AC by activation with phosphoric acid. The effects of the activation temperature and phosphoric acid impregnation on the textural and chemical properties of the adsorbent were investigated. The gas-phase adsorption of nitrogen dioxide and NH_3 onto the palm shell adsorbents was studied. They concluded that phosphoric acid changed or modified the surface chemistry of the adsorbent, due to the formation of acidic oxygen-containing complexes by strong oxidization. These surface functional groups would affect the performance of the adsorbents if used for acidic or basic gases. At high temperatures (600 and 900°C for chemical and thermal activation processes, respectively), fewer micropores were evident, due to pore enlargement and widening, i.e. conversion of micropores to meso- and/or macropores.

Ip et al. (2008) claimed that ACs produced from bamboo, a natural biomaterial, with phosphoric acid, resulted in high surface areas. The effects of the phosphoric acid impregnation ratio, activation temperature and heating rate on the carbon surface area, porosity and mass yield were investigated. Three of these bamboo-derived active carbons (i.e. those with surface areas of 1337, 1628 and 2123 m^2/g) were assessed for their ability to adsorb Acid Red 18 dye from an aqueous solution. They also showed that chemically activated biochars using phosphoric acid had more mesopores comparable to commercially available biochars. The adsorption capacities of two of the selected bamboo derived carbons were much greater than the capacities of the other adsorbents (Ip et al., 2008).

Guo et al. (2005) investigated the adsorption of ammonia (NH_3) onto activated carbons prepared from palm shells impregnated with sulphuric acid. The effects of the activation temperature and acid concentration on pore surface area development were studied. The

relatively large micropore surface areas of the produced ACs suggest their potential application in gas adsorption. Adsorption experiments at a fixed temperature showed that the amounts of NH_3 adsorbed onto the chemically activated carbons, unlike those prepared by CO_2 thermal activation, were not solely dependent on the specific pore surface areas of the adsorbents.

Lee and Choi (2000) used chemical activation of high sulphur (7%) petroleum cokes with alkali metal compounds. They activated the raw material in the temperature range of 400–600°C. Surface areas increased up to 1350 m^2/g for the ACs from petroleum cokes, but were lower than those of coal at the alkali/coke ratio of 4. KOH proved to be more effective than sodium hydroxide for the development of surface area (Lee and Choi, 2000).

Barnard in 2011 used petroleum coke for producing ACs with KOH activation for NA uptake. The AC production involved grinding and sieving petroleum coke particles to a size of 44–149 μm. Petroleum coke and KOH were mixed in a 1:3 w/w ratio. The effect of temperature on production of ACs was studied at a constant KOH / petroleum coke ratio. The temperature varied between 500 to 800°C for a period of 2 hours. They concluded that the trend of temperature versus uptake capacity was a curve and that the optimal temperature was 700°C. The uptake of NA for this sample was 32.8 mg/l for an initial point 41 mg/l of solution (Barnard, 2011).

2.9 Physical Activation

In physical activation, producing AC from raw material has two steps, carbonization and activation. In carbonization the volatile material like O, H, N, and S species from the raw materials are pyrolysed producing a solid char but it is necessary to increase the surface area of the char to make it effective as an adsorbent. Processes for increasing surface areas and porosity have been frequently investigated by various researchers to provide adsorption capacity for

industrial purposes. Although, as already highlighted, process conditions such as final temperature, heating rate, etc. influence biochar's physical structure, commercially viable internal surface areas are almost always generated in high C-containing biochar precursors through physical or chemical activation (Lehmann and Joseph, 2009). In the following, biochar production and physical activation will be discussed.

2.9.1 Biochar Production

Biochar production (i.e. the carbonization step) is the first step in producing AC. Carbonization is a pyrolysis step in which volatile compounds are distilled off the carbonaceous material. In this stage, the raw materials are carbonized in an inert atmosphere at a temperature between 400 and 800°C. This produced material, called biochar has rudimentary pores. After this stage, activation is performed to achieve higher surface areas

Lehman and Joseph (2009) defined biochar as the carbon-rich product obtained when biomass, such as wood, manure or leaves, is heated in a closed container with little or no oxygen present. In other words, biochar is produced during the thermal decomposition of organic material under a limited supply of oxygen at relatively low temperatures (<700°C). In their book, Lehman and Joseph stated that biochars can be produced using different process conditions, such as the heating rate of the feed stock, the final temperature of the charring process, the pressure of the carbonization process, the amount of air or steam added to the reactor, and the temperature of the biochar at the point of addition.

There is very little information in the literature on the optimization of carbonization conditions before activation. One of these rare studies is the research of Lua et al. (2004), who investigated the effect of carbonization in fixed activation conditions. They varied the heating rate, the final temperature, the holding time at the final temperature and the nitrogen flow rate, in

order to determine the optimal conditions for highest BET surface area in ACs. Their raw material was pistachio-nut shells.

Several studies have investigated the carbonization step. Many of these researches were focused on the production of bio-oil rather than biochar. Ozçimen and Ersoy-Mericboyu (2010) employed apricot stones, hazelnut shells, grape seeds and chestnut shells as the raw material to obtain bio-oil and biochar. They showed that biochar production was maximized at a very low heating rate. As the heating rate increased, the yield of biochar decreased and the yield of bio-oil increased. The BET surface areas of the biomass and biochar samples varied between 5.8421 and 10.5881 m^2/g and 0.6717 and 14.6836 m^2/g, respectively. They concluded that, in comparison with raw biomass samples, a decrease in volatile matter and an increase in fixed carbon content were observed for biochar samples. The presence of volatile matter in biochar samples showed incomplete thermal degradation during carbonization.

Ozçimen and Ersoy-Mericboyu (2008) also conducted carbonization experiments on grape seed and chestnut shell samples to determine the effects of the temperature, sweep gas flow rate and heating rate on the biochar yield. Statistical design methods were applied in the design of experiments. The carbonization conditions were selected according to a two-level factorial design matrix considering the following variables: temperature (500°C and 600 °C), N_2 flow rate (0 and 1000 cm^3/min) and heating rate (5 and 20 °C/min). It was found that temperature had the strongest effect on the biochar yields, compared to those of the N_2 flow rate and heating rate. They determined that there was a direct relationship between the increase of all variables and decreased biochar yield. They also showed that any raw material with more fixed carbon will result in a higher yield.

2.9.2 Activation Stage

Physical activation, which is carried out most frequently in industry, is obtained when the initial pyrolysis reactions, occurring in an inert atmosphere at moderate temperatures of 400–800°C, are complemented by a second stage in which the resulting biochars are subjected to a partial gasification at a higher temperature (usually >900°C) with oxidizing gases, such as steam, CO_2, air or a mixture of these. This produces final products with well-developed and accessible internal pores (Lehmann and Joseph, 2009). Steam or CO_2 are mainly used as the activation agents in physical activation; and, depending on which agent is used, the final ACs have different properties.

The use of petroleum coke in the production of ACs was studied by DiPanfilo and Egiebor (1996). They used steam to physically activate fluid petroleum coke. The temperature for activation was 900°C with the heating time varied between 2 and 6 hours. The total pore volume of produced ACs was 60% mesopores, and the total surface area ranged from 118 to 319 m^2. The burn off of AC was proportional to the heating period.

In Small (2011), extensive physical activation experiments were conducted using a combination of environments (CO_2, CO_2 + steam, N_2 + steam) on petroleum coke from a delayed coker. Small varied other activation conditions, including the steam flow rate (0.3-0.5 mL/min), the activation time (2-6 hours) and the activation temperature (800 to 900°C). In the case of CO_2 and steam, the ACs produced at 900°C had a range of physical characteristics: total surface area was from 426 to 578 m^2/g, with mesopores accounting for 37-48% of the total pore volume, and the carbon burn off ranged from 44.2-58.8%.

Nabais et al. (2008) used coffee endocarp as the precursor for producing AC. They showed that CO_2 activation lead to a higher BET surface area than steam for the same degree of

burn off. Activation by both methods produced ACs with small external areas and microporous structures, with very similar mean pore widths. Carbonization was carried out by heating to 600°C at a rate of 10°C min^{-1} under a constant N_2 flow of 85 cm^3/min^{-1} and maintained for 30, 60 or 120 minutes. Their activation condition was a CO_2 flow of 85 cm^3/min at 700°C, with different times to reach burn offs between 14 and 45%.

Aworn et al. (2009) prepared AC from corn cobs with CO_2 activation. They carried out activation at different temperatures (300–800°C) and showed that AC would have a higher surface area but lower yield with increasing activation temperature.

Tseng et al. (2006) conducted research to study the adsorption ability of KOH etchings and CO_2 gasification for the adsorption of dyes and phenols from water. They proposed a new method for producing AC.

Maciria-Agullria et al. (2004) produced AC fibres physically with steam and CO_2 and chemically with sodium hydroxide and KOH. The purpose of their study was a comparison of physical and chemical activation. They figured out that, by using chemical activation, it is possible to obtain similar, or even higher, porosity than by physical activation. Chemical activation had two important advantages: (1) a much higher yield (27-47% for chemical activation and 6% physical activation for 2500 m^2/g AC fibres), and (2) the surface of the fibres prepared by chemical activation was less damaged than by physical activation.

In the literature, the activation temperature with CO_2 was generally between 700 and 1000°C (Rodríguez-Reinoso and Molina-Sabio, 1992) and, the most important variables in the gasification process, from the point of view of porosity development, have been shown to be the activating agent, the final burn off reached, and the presence of inorganic impurities that catalyze

or inhibit the gasification reaction. Burn-off is an index for the extent of reaction, described in further detail in Chapter 3.

Rodríguez-Mirasol et al. (1993) also used CO_2 for producing AC at 800°C. Both chars showed comparable behaviour regarding the evolution of porous structure. Activation increased both the total and narrow microporosity, and a substantial mesoporosity was developed. At high burn-off levels, macroporosity also became significant. BET surface areas in the vicinity of 1,300- 1,400 m^2/g were achieved at burn-off levels of around 70-75%, which correspond to overall carbon-to-lignin yields of about 10-11% .

Lua and Guo (2000) prepared AC with one-step CO_2 activation. Their raw material was oil palm stones. Their experimental results showed that the particle size of the starting material and the heating rate appeared to have no significant effects on the BET surface areas of the ACs; however, the CO_2 flow rate had a significant influence. Increasing the heating rate resulted in slight reductions in the micropore surface areas. The BET and micropore surface areas of the ACs were also found to be dependent on the activation temperature and the hold time. The optimal conditions for activation were an activation temperature of 850°C and a hold time of 2 hours, at which maximum BET and micropore surface areas were found – 1410 and 942 m^2/g, respectively. The pore size distributions of the AC also confirmed these conditions.

Lua and Guo (2001) produced microporous AC with CO_2 activation. The effects of CO_2 activation conditions (i.e. activation temperature and hold time) on the characteristics of the AC, namely the composition, porosity, hardness and internal pore surface area, were investigated in order to optimize preparation parameters. Carbonization was done using purified nitrogen (99.9995% purity) as a purge gas at a flow rate of 150 cm^3/min. The furnace temperature was increased from room temperature to 873 K and held at this temperature for 3 hours. The resulting

chars were then activated at 500-900°C for 10-60 minutes under a CO_2 (99.998% purity) flush at a flow rate of 100 cm^3/min. In both cases, a heating rate of 10 °C/min was used.

Daud et al. (2000) prepared AC and studied the effects of the carbonization temperature on pore development in palm-shell AC. Activation of chars that were prepared at 500, 800 and 900°C was performed with steam at 820°C in a fluidized bed reactor. The ACs prepared from high-temperature char had a significant volume of micropores. Only a small amount of mesopores developed in the initial stage of activation. However, as the level of the burn off increased, a rapid development of mesopores was observed.

Jia and Lua (2008) produced ACs with steam activation. Oil palm shells were converted into ACs by vacuum or nitrogen pyrolysis, followed by steam activation. The effects of the pyrolysis environment, temperature and hold time on the physical characteristics of the ACs were studied. The optimal pyrolysis conditions for preparing ACs for obtaining high pore surface area were vacuum pyrolysis at a temperature of 675°C and 2 hours of hold time, at which the BET and non-microporous surface areas were 988 m^2/g and 273 m^2/g, respectively. However, when pyrolyzed in a nitrogen stream, the ACs yielded BET and non-microporous surface areas of 794 m^2/g and 157 m^2/g, respectively, at a pyrolysis temperature of 750 °C and a hold time of 2 hours. In a vacuum environment, the volatiles released from the oil-palm shells during pyrolysis could be quickly removed to reduce pore blockage to steam during the subsequent activation process. The activation conditions were fixed at a temperature of 900°C and a hold time of one hour. Using the ACs produced at optimal pyrolysis conditions, the maximum phenol adsorption capacity was 166 mg/g of AC. For all the phenol adsorption tests conducted, the adsorption capacity was found to be linearly proportional to the BET surface area of the AC.

In Lua and Jia (2009), steam-activated carbons from oil palm shells were prepared and used in the adsorption of phenol. The largest BET surface area of the AC was 1183 m^2/g with a total pore volume of 0.69 cm^3/g using N_2 adsorption at -200° C .The experimental tests on the adsorption of phenol by the ACs were carried out in a fixed bed. The effects of the operation conditions of the fixed bed on the breakthrough curve were investigated.

(DiPanfilo and Egiebor, 1996) used delayed petroleum coke as the precursor of AC. They used a two-step physical activation with steam. The activation of the petroleum coke was evaluated using a fixed bed reactor involving carbonization and activation steps at a temperature of 850°C using steam as the activation medium. They claimed that the maximum surface area was achieved in an activation period of 4 hours. Increasing the activation period to 6 hours showed a decrease in the surface area. They tested their produced ACs in the adsorption of colour and chlorinated organics reduction from pulp mill wastewater. They also showed that there was a direct relation between adsorption and surface area.

Teng and Lin (1998) used Australian bituminous coals as the raw material for producing ACs. The preparation process consisted of carbonization followed by activation with CO_2. Their study focused on the oxygen content of AC. They found that the oxygen content in bituminous coals had a significant influence on the surface structure of the resulting chars and the ACs with CO_2 activation. The BET surface area of the char increased with the oxygen/carbon ratio of the raw coal. They suggested that the oxygen functional groups promoted the cross-linking between coal structures, which decreased the thermoplastic property during carbonization of a coking coal. They also claimed that the decrease in the surface area in high burn off was related to an increased ratio of ash. The average pore diameter of the ACs from the same coal increased as the

activation temperature was elevated. However, there was no obvious trend for the variations in the surface area and pore volume with the activation temperature.

Teng et al. (1996) demonstrated that the oxidation of bituminous coal precursors had a significant influence on the surface structure of the resulting chars and the ACs upon CO_2 activation. The oxidation resulted in increases in the specific surface areas and pore volumes of the resulting ACs, whereas the average pore diameter of the carbons decreased. The rate of the CO_2 activation was higher for the carbon from an oxidized coal than that from a corresponding unoxidized coal. The increase in the activation rate due to the oxidation could be, at least partially, attributed to an increase in surface area. The oxidation of the coals could also produce a char structure that is more accessible for CO_2 penetration during activation.

In the case of steam or CO_2 at atmospheric pressure, the kinetically controlled regime is below approximately 900°C; hence, this step is usually performed at 750–900°C. The mechanisms of these gasification reactions are different and have been studied extensively (Walker et al., 1959; Yang, 1984). A main function of gasification is the widening the pores, creating large mesoporosity.

The effect of activation temperature on physical activation was evaluated in several studies. In almost all cases, higher burn off was achieved as the activation temperature increased. This trend can be attributed to faster gasification reaction due to higher temperature

The effect of activation temperature on surface area was not as straightforward as that of the burn off. In some studies, higher surface area was achieved as the temperature increased such as in the work of Daud et al (2000) where these researchers stated that this effect was due to increasing volume of precursor. On the other hand, some research showed that the surface area decreased as the temperature increased. Interestingly, this effect was shown in an extensive burn-

off region. This effect may be attributed to an extensive carbon / gasifier agent reaction leading to an ash rich material.

2.10 Objectives and Research

The primary objective of this research was the preparation of an appropriate AC for the adsorption of naphthenic acids (NA) by means of physical activation. The raw material was sawdust from a common mill in Calgary. The main source of this sawdust was pinewood, which is abundant in Alberta. The method used for the production of AC from biomass was physical activation with CO_2 activation. The physical activation was comprised of two stages: carbonization and activation.

The carbonization (biochar production) was also studied, based on experimental design. The effects of the activation temperature on the burn off and surface area of the produced ACs was studied. The relationship between the activation temperature and the surface area of the AC was also investigated. Chemical and physical activation was compared, based on their characteristic properties, such as elemental analysis, surface area and microposity area.

Finally, an adsorption test was performed to investigate the adsorption ability of the produced ACs. With equilibrium data, the isotherm was revealed.

Chapter Three: **Experimental Equipment and Procedure and Theory**

In this research project, activated carbon was first produced from biomass and then used for adsorption of naphthenic acid in the aqueous phase. The produced carbon from biomass, known as biochar, was subjected to physical activation in order to increase its surface area and to enhance its adsorption capacity. Physical activation consists of two steps, carbonization and activation. In the carbonization step, the effect of final temperature, heating rate and time on the quality and yield of the produced biochar were studied. Carbon dioxide was chosen as the primary agent for physical activation of the biochar. In order to evaluate the effect of temperature and biomass particle size on the produced carbon, various samples were prepared, and their adsorption capacity was measured. For comparison, chemically AC was also produced using phosphoric acid as the activating agent.

The measured parameters included the yield, reaction surface area, adsorption capacity and elemental analysis. In addition, the structure of the AC was determined by X-ray diffraction and scanning electron microscopy. Having thermal gravimetric analysis data allows for determination of reaction kinetics for both carbonization and activation. Yield from the reactor can be verified with TGA data.

In this chapter, biochar production methods and the adsorption apparatus are discussed in detail.

3.1 Raw Material Biomass

The biomass selected for this research was a mixture of sawdust from different types of wood obtained from a waste wood recycling company. This biomass was the same as that used by Salehi et al (2010).

The feedstock was initially dried, crushed in a crusher and then sieved to different mesh sizes in ranges of < 590 μm, 590-1000 μm and 1000-1400 μm. For the sake of consistency, the biomass was heated overnight in an oven at 100°C to remove any residual moisture. The ultimate (C, H and N analysis) and proximate analyses of the biomass are shown in Table 3.1. Proximate analysis was done using TGA based on ASTM D3172 - 07a to determine the fixed carbon, ash, volatile and moisture content. Ultimate analysis was done for determining the total carbon, nitrogen, hydrogen and oxygen of material regardless of their nature. Due to the low sulfur and ash content of the feedstock, these have not been included in the tabulation.

Table 3.1 Proximate and ultimate analysis of biomass

	as received	dry basis	dry, ash free
Proximate analysis wt (%)			
Moisture	5.96		
Ash	1.46	1.55	
Fixed carbon	11.42	12.14	12.34
Volatile	81.15	86.30	87.66
Ultimate analysis wt (%)			
Carbon	47.37	50.37	51.17
Hydrogen	6.03	6.41	6.51
Nitrogen	2.40	2.55	2.59
Oxygen	36.78	39.11	39.73

3.2 Biochar Production Method

In the physical production of AC, biomass should be converted to a material with higher carbon density (Lehmann and Joseph, 2009). This is normally achieved by distilling off any volatile material in the biomass. Pyrolysis, the process of heating organic materials in an inert atmosphere, was used to achieve this goal (Lehmann and Joseph, 2009).

The biochar production was performed in a horizontal stainless steel fixed-bed tubular reactor (internal diameter of 1.9 cm, external diameter of 2.2 cm, length of 50 cm) in an ultrapure nitrogen (N_2) flow (99.999%), externally heated by a 1200 W electrical tube furnace.

In each experiment, 10 grams of dried biomass were placed in the furnace. All of the experiments were done at a constant N_2 flow rate of 80 ml/min. Heating ramp, final temperature and residence time at the final temperature were 10 °C/min, 550 °C and 2 hours respectively. After the allotted time at the final temperature had passed, the reactor was turned off and allowed to cool down. After the furnace temperature reached ambient condition, the residue (biochar) was collected and weighed.

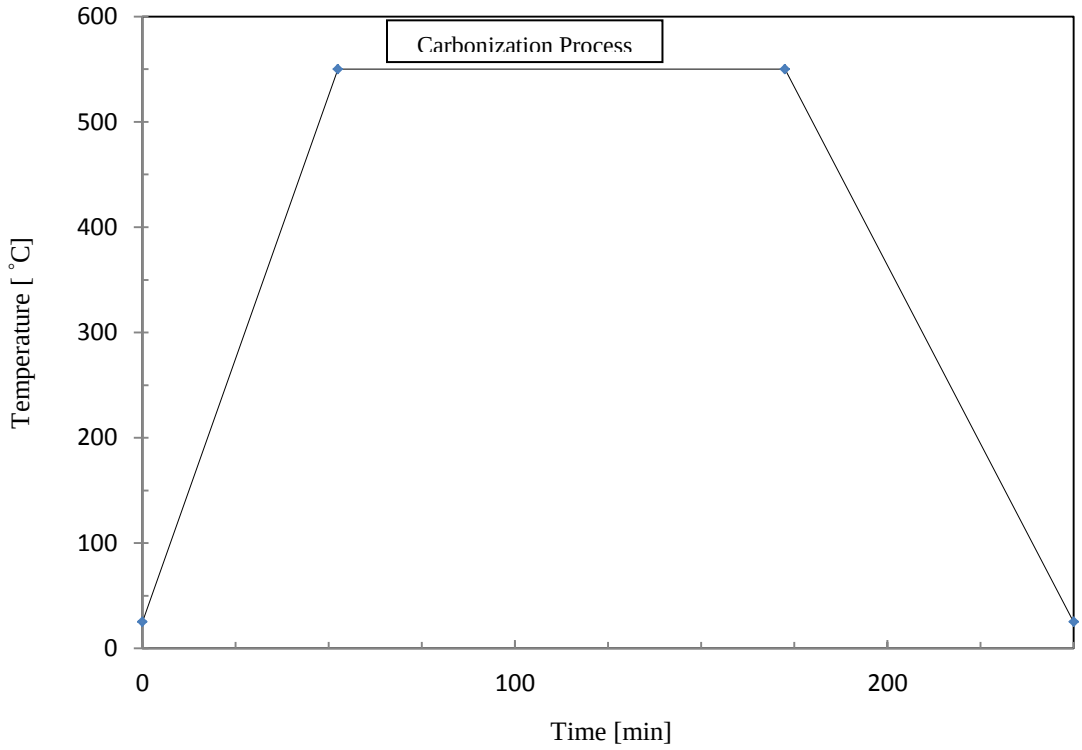

Figure 3.1 Temperature versus time for carbonization step

The furnace conditions involved three variables: the heating rate, the final temperature and the residence time which is defined as the time that the sample is heated at the final temperature. The N_2 flow rate was held constant at 80 ml/sec. Figure 3.1 shows a plot of the temperature versus time sequence employed for a particular sample. Table 3.2 describes the various conditions used for producing the biochars.

Table 3.2 Produced biochar's conditions

Experiment No.	Heating Rate (°C/min)	Final Temperature (°C)	Residence Time (hr)
1	5	450	0.5
2	5	550	1
3	5	650	1.5
4	5	700	2
5	10	450	1
6	10	550	0.5
7	10	650	2
8	10	700	1.5
9	15	450	1.5
10	15	550	2
11	15	650	0.5
12	15	700	1
13	20	450	2
14	20	550	1.5
15	20	650	1
16	20	700	0.5

3.2.1 Physically Activated Carbon Production

After the production of biochar, it was activated using CO_2 in the same reactor. The purity of CO_2 in this study was 99.999%. A photograph of the experimental apparatus is shown in Figure 3.2.

In order to investigate the effect of temperature on activation carbon, temperatures of 700 to 900°C were used to activate the biochar. The whole process from raw material to AC is shown in Figure 3.3.

Figure 3.2 Carbonization and activation setup

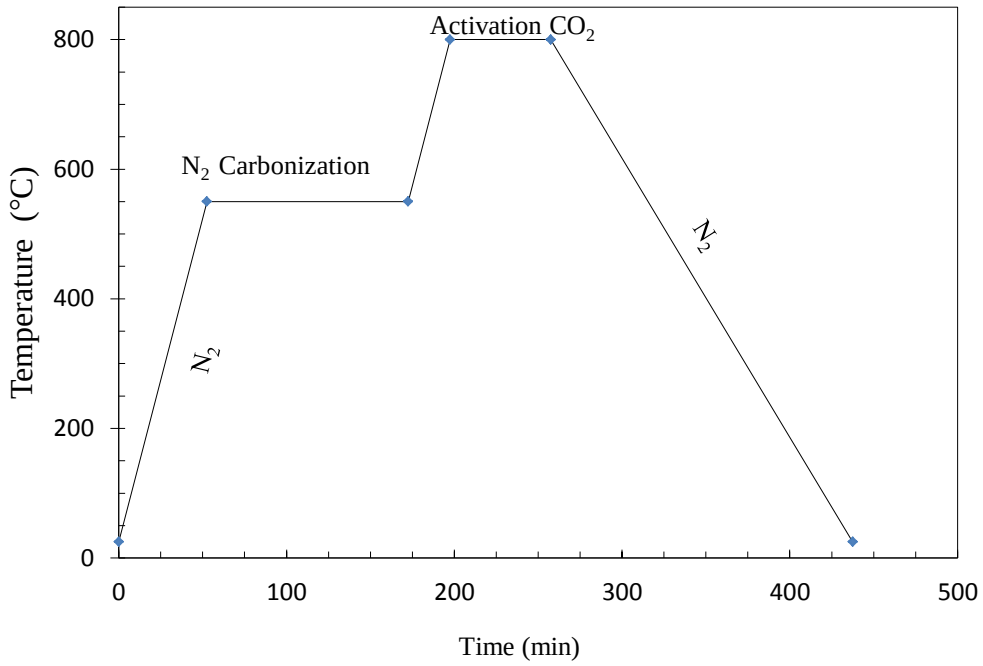

Figure 3.3 Temperature versus time for producing activated carbon

3.3 Chemically Activated Carbon Production

As mentioned earlier, chemical activation is another way to produce AC. For this research, phosphoric acid was used as the activation agent. The sawdust sample was crushed to 590 µm and then dried overnight in an oven at 100 °C. A predetermined amount of phosphoric acid acquired from BDH company with a purity of 85% was used to impregnate the biomass. The biomass-acid ratio was 1/1. The acid was poured in a container and diluted, and then mixed with biomass. The mixture was placed in a stirrer for 5 hours and then dried in an oven overnight at 100°C. The dried impregnated biomass was then placed in a 1 in. tubular reactor inside a furnace. A quartz holder was also used to pack the reactor. The final temperature was set at 550°C, with a ramp up of 10°C/min and held at the final temperature for 2 hours. The reactor was cooled to ambient temperature and the AC was collected. Because the produced AC was impregnated with acid and the acid can reduce the porosity of the AC, it was washed with de-

ionized water to establish a neutral pH of 7 then dried overnight. This sample was designated CA to reflect the fact that it was a chemically AC sample. All produced activated carbon and their conditions are shown in Table 3.3.

Table 3.3 Temperature versus time for producing activated carbon

Sample Name	Mesh size	Carbonation Step	Activation step
N1	590-1000 µm	550 ^{o}C, 2hr, 10 C/min	800 ^{o}C,1 hr CO_2
N2	590-1000 µm	550 ^{o}C, 2hr, 10 C/min	825 ^{o}C,1 hr CO_2
N3	590-1000 µm	550 ^{o}C, 2hr, 10 C/min	850 ^{o}C,1 hr CO_2
M1	1000-1400 µm	550 ^{o}C, 2hr, 10 C/min	800 ^{o}C, 1 hr CO_2
M2	1000-1400 µm	550 ^{o}C, 2hr, 10 C/min	825 ^{o}C, 1 hr CO_2
M3	1000-1400 µm	550 ^{o}C, 2hr, 10 C/min	850 ^{o}C, 1 hr CO_2
AC1	<590 µm	550 ^{o}C, 2hr, 10 C/min	700 ^{o}C, 1 hr CO_2
AC2	<590 µm	550 ^{o}C, 2hr, 10 C/min	750 ^{o}C, 1 hr CO_2
AC3	<590 µm	550 ^{o}C, 2hr, 10 C/min	800 ^{o}C, 1 hr CO_2
AC4	<590 µm	550 ^{o}C, 2hr, 10 C/min	825 ^{o}C, 1 hr CO_2
AC5	<590 µm	550 ^{o}C, 2hr, 10 C/min	850 ^{o}C, 1 hr CO_2
AC6	<590 µm	550 ^{o}C, 2hr, 10 C/min	900 ^{o}C, 1 hr CO_2
CA	<590 µm	No Carbonization step	550 ^{o}C, 2hr N_2

3.3.1 Yield

As a result of the carbonization process, some volatiles are driven off the biomass. Therefore, at the end of this process, a reduction of weight relative to the original sample is observed. Yield is the term to describe the percentage of the remaining weight over the initial weight and can be an indicator of the extent of reaction. The yield formula is:

$$Yield = \frac{Weight\ of\ produced\ biochar}{Weight\ of\ intial\ biomass} \times 100 \qquad 3\text{-}1$$

3.3.2 Burn-Off

In the activation process, which is basically a gasification reaction, the pore size is widened, and some weight is lost. Burn-off is defined by the weight of remaining biochar

following activation in relation to the weight of the biochar initially as shown in the equation below. Burn off, determined on a dry weight basis, is a common measure used for the activation process (Aworn et al., 2009, Johns et al, 2009). The activation burn-off can be calculated from experimental data as:

$$Burn - off = 1 - \frac{final\ weight\ of\ produced\ activated\ carbon\ value}{initial\ biochar\ weight} \quad 3\text{-}2$$

Calculation of the burn-off is systematic for physically AC, because the weight of biochar can be easily obtained. For chemically AC, the burn-off is defined as the mass of reacted carbon relative to the mass of the fixed carbon (FC) in the sample before activation and is calculated as (Fukuyama and Terai 2008):

$$Burn - off\ (\%) = (1 - \left(\frac{The\ weight\ of\ sample\ after\ activation}{The\ weight\ of\ FC\ in\ the\ sample\ before\ activation}\right)) \times 100 \quad 3\text{-}3$$

3.4 Micrometric Tristar

For measuring the BET (Brunauer, Emmett, Teller) surface area, pore size distribution, average pore size and total pore volume, the Micrometric Tristar II analyzer was used. This device has three separate ports; therefore, three samples could be analyzed simultaneously.

Pore sizes were defined according to three main categories: micropores (pore diameter < 2 nm, 20 Å), mesopores (2-50 nm, 20-500 Å) and macropores (pore diameters > 50 nm, 500 Å) (Do, 1998). The mean of each parameter (x_{avg}) – total surface area, total pore volume, micropore area was calculated. In addition, the standard error (S.E.) or standard deviation in each parameter was calculated by performing three runs in the Tristar analyzer:

$$S.E. = \sqrt{\frac{1}{n-1}\sum_{i=1}^{n}(x_i - x_{avg})} \quad 3\text{-}4$$

where n is number of runs done in the Tristar device, and x_i is the value of particular parameter.

In this work, N_2 was used for estimating surface area, pore size distribution, average pore size and total pore volume of ACs. The cryogenic temperature of N_2 is 77 K, which is consistent with the temperature of the liquid nitrogen bath. The sample was then exposed to the adsorption gas in a specific pressure range. The idea was to determine the isotherm in the specific range. The BET equation could then be used to find the surface area and other parameters such as mesoprosity and average pore size.

The pressure range in this apparatus was set at 0.01-0.95 P/P_0, where P_0 is the saturation pressure and P indicates the equilibrium pressure. The isotherm is the relationship between the adsorbed gas (N_2) on the solid surface and P/P_0. As the adsorption of N_2 or CO_2 molecules continues, micropores are filled first and then the larger pores are occupied (mesopores and macropores) by capillary condensation (Do, 1998).

Before doing the adsorption test on the surface, the surface should be polished and clean. Therefore, outgassing was done to polish the surface of the ACs or biochar samples.

In the following subsection, the method for outgassing, BET theory, and measurements of the pore size distribution, total pore volume and average pore size are discussed.

3.4.1 Outgassing

The purpose of outgassing is the elimination of any adsorbed gas on the surface of a solid. One of the common gases adsorbed on the surface is water vapor, which can block narrow pores from gas adsorbents and could possibly change surface properties (such as heat of adsorption), leading to erroneous data measurement in the instrument.

Outgassing for this work was conducted at 423 K, under the flow of ultra-high purity N_2 (Praxair, Ni5.0 UH-T) and high vacuum. As per the recommended operation of the device, the amount of sample placed in the cell was in the range of 5-10 m^2 for measuring the surface area

and other parameters. The ACs had surface areas of 400-1200 m^2/g; therefore, the weight of the samples was set in the range of 0.100-0.200 g and placed in sample cells.

For these experiments, a 2.5 L Dewar flask was filled with liquid nitrogen up to a certain marker, and the flask was placed on its stand in the Tristar analyzer. During the experiments, the sample cells were immersed in the liquid nitrogen to reach the temperature of 77 K. Through the manifold in the device, the pressure of N_2 was fixed within a range of 0.01 and 0.95 P/P_0. The adsorption of N_2 was measured at 84 different points.

After weighing the cells, they were placed in the apparatus for outgassing. After the samples were outgassed, the sample cells were weighed again. The weight of sample was determined by subtracting the empty cell weight from that of the whole cell after outgassing.

3.4.2 Surface Area Measurement

The reaction surface area is one of most important parameters for a solid and is expressed in surface area per gram. There are several methods for calculating the surface area of a sample but the most widely accepted and commonly used is the BET method. The BET theory uses the same assumption as the Langmuir theory, which is that the surface is homogeneous, implying that the adsorption energy is constant over all sites at the surface. Essentially, the Langmuir theory is based on monolayer molecular adsorption. The adsorbed atoms or molecules are adsorbed at definite, localized sites; and each site can accommodate only one molecule or atom.

The concept of the Langmuir theory is based on the kinetic principle that the rate of adsorption is the same as the rate of desorption. The Langmuir theory can be stated as for gas phase:

$$\frac{V}{V_m} = \frac{bp}{1+bp} \qquad 3\text{-}5$$

Where V is the volume of gas, P is the pressure, V_m is the volume of the adsorbed chemical required to form a monomolecular layer, and b is a constant.

In the BET theory, the assumptions made are that there is homogeneous surface energy and no interaction among adsorbed molecules and there is no monolayer assumed as in the Langmuir theory. In BET, the Langmuir theory can be applied to each layer; and, the resulting BET equation is expressed by:

$$\frac{P}{V(P_0-P)} = \frac{1}{V_M C} + \left(\frac{C-1}{V_m C}\right)\frac{P}{P_0} \qquad 3\text{-}6$$

Where P is the equilibrium pressure, P_0 is the saturation pressure of the adsorbate at the corresponding temperature of adsorption, V is the adsorbed gas quantity, V_m is the monolayer adsorbed gas quantity, and C is the BET constant. C can be expressed as:

$$C = exp\left(\frac{E_1-E_L}{RT}\right) \qquad 3\text{-}7$$

Where E_1 is the heat of adsorption for the first layer, and E_L is the heat of adsorption for the second and higher layers and is equal to the heat of liquefaction.

Do (1998) stated that the validity of the BET equation is in the range P/Po = 0.05 - 0.3. He also stated that, if the relative pressure is above 0.3, capillary condensation occurs, which is not amenable to multilayer analysis. This knowledge about capillary condensation is used to determine the pore size distribution, as the pressure at which the liquid condenses in a pore depends on the pore size.

A plot of the BET equation versus P/P_o would yield a straight line with a slope of $\frac{(C-1)}{CV_M}$ and an intercept of $\frac{1}{CV_M}$. The famous BET equation is used extensively for the area determination because once the monolayer coverage V_m is known and the area occupied by one molecule is known, the surface area of the solid can be calculated.

Usually, the value of C is very large, because the adsorption energy of the first layer is larger than the heat of liquefaction. The slope is then simply the inverse of the monolayer coverage, and the intercept is effectively the origin. Therefore, very often, that one point alone is sufficient for the first estimate of the surface area.

Once V_m (mole/g) is obtained from the slope, the surface area is calculated from:

$$A = V_m N_A a_m \qquad 3\text{-}8$$

Where N_A is the Avogadro number and a_m is the molecular projected area. For each gas, there is a number, which is 16 (Å/molecule) for N_2. (Do, 1998)

3.4.3 Micropore Surface Area and Micropore Pore Volume

By using the t-plot method, the micro-pore surface area and the pore volume can be measured. The procedure is detailed in the following steps (Do, 1998):

1. A reference non-porous material with similar surface characteristics is chosen to obtain the information on the statistical film thickness as a function of the reduced pressure. The t values for different reference adsorbents as a function of the reduced pressure are available in literature, normally in table form or a best fit equation.
2. The equilibrium data of the amount adsorbed versus the reduced pressure are plotted as the amount adsorbed versus the statistical thickness by using the data of nonporous material in step 1.
3. From the plot of step 2, there are usually two distinct linear regions and two straight lines can be drawn from these two regions. The slope of the first line passing through the origin can be used to calculate the total surface area, while the slope of the second straight line is used to

calculate the external surface area. The intercept of the latter line gives the volume of the micropores.

3.4.4 Pore Size Distribution

The pore size distribution can be determined by the Barrett Joyner Halenda (BJH) method (Do, 1998). The concept of this theory is based on the condensation pressure, through which the pore size radius can be related. During the adsorption cycle, the pore is filled with the adsorbent in a radial fashion; hence, the rise in the adsorbed amount versus pressure is gradual. This method also assumes that there is capillary condensation in these cylindrical pores that have multilayer adsorption on their walls.

3.4.5 Total Pore Volume

The total pore volume can be determined by calculating the volume of the vapor condensed within the walls of the pores. Therefore, the total pore volume is determined at a maximum reduced pressure (P/P_0) of 0.98. The volume of liquid that adsorbed from the vapor phase can be calculated from the following formula:

$$V_{total} = \frac{P_{atm} V_{ads} V_{molar}}{RT} \qquad 3\text{-}9$$

Where P_{atm} is the ambient pressure, V_{molar} is the liquid molar volume of the adsorbate (34.7 cm^3/g for N_2), and V_{ads} is the volume adsorbed at the maximum relative pressure of 0.98.

3.4.6 Average Pore Size

By considering the pore as a cylinder, it is possible to calculate the pore size from the total pore volume and the total surface area observed from the BET analysis. For the total volume of all of the pores, the summation of all cylinders is used. From this data, the average

pore size can be calculated. Therefore, the volume of all pores (V_{total}) is determined using the equation for the volume of a cylinder:

$$V_{total} = \frac{\pi}{4} D^2 h \quad (3\text{-}10)$$

where h represents the height of the cylindrical shaped pore.

The surface area of a cylindrical shaped pore can be determined from the following relation:

$$S_{total} = \pi D h \quad (3\text{-}11)$$

Therefore, rearranging the equation and combining it with the volume of a cylinder, we obtain:

$$V_{total} = \frac{\pi}{4} D \left(\frac{S_{total}}{\pi}\right) = \frac{D S_{total}}{4} \quad (3\text{-}12)$$

Rearranging of the above equation to obtain the average pore diameter gives:

$$D = \frac{4 V_{total}}{S_{total}} \quad (3\text{-}13)$$

3.5 Thermal Gravimetric Analysis

Thermal gravimetric analysis (TGA) is a type of measurement performed on samples to determine changes in weight relative to a change in temperature. Such analysis relies on a high degree of precision in three measurements: weight, temperature, and temperature change. TGA can produce plots of weight versus time or weight versus temperature. With the help of TGA, one can investigate the kinetic reaction and its extent for a given time or temperature. Moreover, with TGA data, yield and other gravimetric parameters can be compared to the reactor's results.

Generally, 10-13 mg of raw biomass is placed in the chamber of a TGA system, which is weighed on a precise balance. The balance weight is recorded with an assigned time interval of 1 second or 1 °C temperature per sample. By collecting the weight, time or temperature of a sample, the TGA plot can be made.

3.6 Adsorption Tests

For investigating isotherms for each AC sample, equilibrium data must first be obtained. In this section, the materials and methods used for the batch adsorption tests are described.

The naphthenic acid used in this study was commercial naphthenic acid (Sigma-Aldrich, technical grade). A mixture of alkylated cyclopentane carboxylic acids was used to model the naphthenic acids (NAs) present in petroleum products and oil and gas wastewater streams. Barnard (2011) used commercial NA, because it is an actual petroleum product.

The measurement of the total organic carbon (TOC), which refers to the amount of carbon bound in an organic compound, is used for quantity. This value is often used as a nonspecific indicator of water quality or cleanliness of pharmaceutical manufacturing equipment (Barnard, 2011). TOC was measured through the use of a Shimadzu TOC-VE TOC analyzer.

TOC can be calculated by subtracting inorganic carbon (IC) from the total carbon (TC). The main source of inorganic carbon is CO_2 carbonic acid salts (Barnard, 2011). In the following subsection, TC and IC measurement theory are discussed.

3.6.1 Total Carbon Measurement

The method to measure TC in the TOC analyzer is the burning of the organic carbon for conversion to CO_2, in order to record the CO_2 production value. Purified air is passed at a certain volumetric rate to an oxidation catalyst column. The temperature of the column is set at 680°C. When the sample is injected in the device, the sample goes through the combustion column and is oxidized or decomposed, thereby generating CO_2. The carrier gas then sweeps the CO_2 and takes it to the dehumidifier to remove the water vapor content and cool the CO_2. After removing the humidity of the gas stream, the carrier gas goes through a halogen scrubber into a sample cell of the non-dispersive infrared detector (NDIR). The NDIR is used to detect the CO_2

concentration and create peaks for quantity measurement by calculating the area below these peaks.

3.6.2 Inorganic Carbon Measurement

The acidified sample is purged with carrier gas (purified air) to convert the IC in the sample to CO_2, which is detected by the NDIR. The sample IC concentration is measured in the same way as TC. The IC is a combination of carbonate and bicarbonate and dissolved CO_2.

The TOC analyzer is calibrated by using the standard solution mentioned in user's manual handbook.

3.6.3 Batch Adsorption

The method used for adsorption was the same as that used by Barnard (2011) for the purpose of comparison with a base case. The volume for adsorption was 20 ml. Adsorption tests were done with different initial concentrations to investigate the presence and profiles of isotherms. With regard to previous studies, the NA concentration in the Athabasca tailings pond water is in the range of ~ 40 - 120 mg/L (Holowenko et al., 2000, Holowenko et al. 2002, Rogers et al., 2002, Allen, 2008a).

As previously discussed, the solubility of NA is dependent on the pH of the water. By increasing the pH, the solubility of NA increases. Without changing the pH of water from its natural value of 7, NA solubility in water is about 40 mg/L (Barnard, 2011).

Preparation of the NA solution involved the following steps. First, a solution of almost 50 mg/L NA was produced by mixing the commercial NA with deionized water. The mixture was put in the sonication apparatus for approximately 3 minutes to hasten the dissolving of NA in the deionized water and to create a more homogeneous solution. In the next step, the deionized water

was added to this solution to a recorded level, and the diluted solution was stirred for at least 3 hours. To make sure the solution was homogeneous, several samples were taken; and, their TOC values were compared to ensure consistency. Sampling was usually done from the bottom, middle and top of the container holding the solution.

The NA / deionized water solution and AC mixture was placed in 20 mL vials. The ratio was set as 1 g of AC to 1 L solution. The vials were placed in an incubating shaker at 298 K and 175 rpm for 24 hours. Three vials were used for each adsorption experiment for each different AC produced at different conditions, with each of the three vials consistent and with the same concentration for each test run, for replication purposes. After this step, the vials were placed in the shaker to agitate for 24 hours at room temperature (23°C). For the standard solution, NA without AC was used with silica sand.

After 24 hours, the samples were taken out of the shaker and the samples were left to settle for an hour before they were filtered using a 0.45 micron nylon syringe filter. The filtrate was then injected into a clean vial for TOC readings. For reproducibility, each of the three vials was tested three times.

Chapter Four: **Results and Discussion**

In this chapter, the data obtained on the production of activated carbon from biomass are presented. Data for the physical activation of biochar using carbon dioxide and the effects of activation temperature and particle size on the final AC product will be presented. The effect of activation temperature on burn-off and surface area will be investigated. Yield, burn-off, N_2 adsorption, and elemental analysis will be used to describe the attributes of the produced AC. In addition, results of naphthenic acid (NA) adsorption are also presented. The effect of surface area and microporosity on adsorption will be presented and discussed. For some produced ACs adsorption tests were done at 5 different initial concentrations of a synthetic solution of NA in de-ionized water. Having the equilibrium for each initial concentration of each produced ACs, the isotherm plots corresponding to each produced AC can be plotted.

4.1 Biochar production results

In the Table 4.1, the experimental conditions and yield for each biochar are shown. Yield can be defined as ratio of final weight to initial weight. Yields are between 20-30 percent, which was expected from raw material analysis.

The data show that as heating ramp and temperature decrease, yield increases. The relationship between heating rate, final temperature and residence time with yield is inversely proportional. The same result was shown in Ozçimen and Ersoy-Meriçboyu (2008). It seems that higher temperature will lead to lower yield because volatiles will distillate off. At longer times volatiles are also exposed more to the heat. Heating ramp showed the same trends as final temperature and residence time.

Table 4.1 Produced biochars and their yield

No. Experiment	Heating Rate (°C/min)	Final Temperature (°C)	Residence Time (hr)	Yield %
1	5	450	0.5	30.86
2	5	550	1	27.92
3	5	650	1.5	27.40
4	5	700	2	26.0
5	10	450	1	27.765
6	10	550	0.5	27.74
7	10	650	2	25.92
8	10	700	1.5	25.65
9	15	450	1.5	29.33
10	15	550	2	25.16
11	15	650	0.5	25.85
12	15	700	1	24.78
13	20	450	2	27.86
14	20	550	1.5	25.56
15	20	650	1	24.83
16	20	700	0.5	24.95

The yield in the present study compared to the work of Salehi's (2011) was higher because in Salehi's studies, fast pyrolysis was used in fixed and fluidized beds and yields were in the range of 10 to 20 percent. Yield variation in Salehi (2011) may be attributed to the use of variable heating rates (5-20 °C/min).

Ozçimen and Ersoy-Meriçboyu (2008) also reported that temperature has the strongest effect on the biochar yield. Biochar yields were around 45 to 58 percent for grape seed and chestnut. At higher temperatures, the yield of produced biochar decreases. The reason for this phenomenon is that the secondary decompositions associated with high carbonization temperatures occur. This type of thermal degradation of biomass (lingocellulosic) occurs when the three main parts (hemicelluloses, cellulose and lignin) of biomass are degraded. At temperatures between 200-260 °C, the hemicelluloses are the first to degrade, followed by the cellulose at 270-350 °C and finally the lignin pyrolizing at temperature in the range of 350-600 °C. Ozçimen and Ersoy-Meriçboyu (2008) have also shown that lower biochar yields were obtained at the higher heating rate. They explained that the higher heating rates result in increasing the rate of volatile matters evolution. In addition, higher heating rates decrease the rates of subsequent chemical reactions and conversions. Therefore, an increase of heating rate during pyrolysis results in both an increased reaction rate and a higher concentration of volatile matter released during pyrolysis, resulting in a lower yield of biochar.

Table 4.2 Carbon content of produced biochar

RUN. NO	WEIGHT (Wt.%)	Carbon (Wt.%)	Hydrogen (Wt.%)	Nitrogen (Wt.%)	Sulfur (Wt.%)
C1	1.795	78.18	3.33	3.13	0.49
C1R	2.404	78.98	3.39	3.13	0.49
C2	2.442	83.60	2.61	2.69	0.40
C2R	1.568	83.21	2.64	2.71	0.52
C3	2.054	85.0	1.67	2.43	0.28
C3R	1.586	85.92	1.66	2.46	0.30
C4	1.661	85.10	1.19	2.23	0.23
C4R	1.520	85.34	1.16	2.22	0.27
C5	1.688	76.55	3.60	2.54	0.59
C5R	1.567	76.86	3.61	2.59	0.60
C6	1.924	80.42	2.49	2.75	0.39
C6R	1.891	81.04	2.54	2.77	0.44
C7	1.748	85.39	1.48	2.48	0.27
C7R	2.357	85.67	1.52	2.34	0.26
C8	1.514	86.51	1.17	2.33	0.23
C8R	1.839	86.98	1.17	2.32	0.19
C9	2.048	77.49	3.22	2.87	0.54
C9R	1.963	77.99	3.09	2.86	0.49
C10	1.514	84.46	2.43	2.76	0.43
C10R	1.967	84.98	2.40	2.84	0.36
C11	1.543	85.56	1.76	2.46	0.33
C11R	2.205	84.97	1.71	2.54	0.30
C12	2.146	85.30	1.28	2.25	0.23
C12R	2.159	86.30	1.28	2.27	0.20
C13	2.431	79.33	3.13	3.85	0.49
C13R	1.580	78.45	3.14	3.03	0.53
C14	2.436	82.0	2.31	2.76	0.36
C14R	1.640	83.70	2.41	3.03	0.41
C15	2.235	85.23	1.57	2.58	0.28
C15R	1.581	85.83	1.58	2.48	0.27
C16	2.442	73.12	1.13	2.16	0.21
C16R	1.751	87.17	1.30	2.41	0.25

The quality of the produced biochar is another important factor and it may be defined by the carbon content of the biochar. Elemental analysis data for 16 samples are shown in Table 4.2. The carbon contents of produced biochars are in the range of 70-85%. It seems there is no obvious relationship between heating rate, final temperature and residence time with carbon content of produced biochar. It is worth mentioning that results for sample C16 and sample C16R are not consistent and almost 14% error was observed. In order to get a more precise result the related experiments need to be repeated.

4.2 Physical and Chemical Activation

In this section, the results of physical activation and chemical activation are shown in detail. Effect of activation temperature on different features of AC such as surface area and burn-off will be discussed.

4.2.1 Burn-off and BET Surface Area versus Activation Temperature

In order to investigate the effect of particle size and activation temperature on the properties of AC, 3 different particle sizes at various activation temperatures were used during the activation stage. Yield of carbonization and burn-off are shown in Table 4.3.The AC series consists of physical activation with CO_2 at activation temperatures from 700-900°C. For M and N series, which were 590-1000 µm and 1000-1400 µm respectively, activation temperatures were 800, 825 and 850°C.

In Figure 4.1 burn-off of AC series are plotted versus activation temperature. As can be seen, as the temperature is increased, burn-off also increases. For AC series where the particle size is less than 590 µm, burn-off was between 20-80% for a temperature range of 700 to 900°C.

For M and N series, which were 590-1000 µm and 1000-1400 µm respectively, activation temperature range was 800 to 850 °C. The burn-off for this range was between 27-56%.

Notably, the burn-off was quite similar for all 3 different particle sizes for any activation temperature. The effect of mesh size on burn-off and yield was not significant. However, temperature is shown to have a large impact on the activation process in terms of yield.

The effect of activation temperature on burn-off was consistent with the literature, although the burn-off was higher than what was reported (Teng and Lin, 1998) (Gergova and Eser, 1996). High burn-off may be attributed to the type of raw material and fixed carbon content of the raw material. As the temperature increased, the yield decreased. The low yield was attributed to the low fixed carbon and the high percentage of volatile material in the raw material.

Interestingly, burn-off and surface area for all three different mesh sizes at the same activation temperature were almost the same. The discrepancy can be due to experimental error. The effect of particle size was studied in Lua and Guo in 1999, and they have shown that the particle size did not have a significant effect on the properties such as surface area and yield of produced AC.

Table 4.3 Produced activated carbon and their features

Sample Name	Particle size	Carbonation Step	Carbonization Yield (%)	Activation step	BET surface(m^2/g)	Burn-off(%)	Yield base on initial biomass
N1	590-1000 µm	550 ^oC, 2hr, 10 C/min	25.7	800^oC,1 hr CO_2	663	27.05	18.20
N2	590-1000 µm	550 ^oC, 2hr, 10 C/min	25.7	825^oC, 1 hr CO_2	720	46.30	13.80
N3	590-1000 µm	550 ^oC, 2hr, 10 C/min	25.7	850 ^oC,1 hr CO_2	507	66.69	8.56
M1	1000-1400 µm	550 ^oC, 2hr, 10 C/min	25.9	800 ^oC,1 hr CO_2	690	33.94	17.11
M2	1000-1400 µm	550 ^oC, 2hr, 10 C/min	25.9	825 ^oC, 1 hr CO_2	731	55.21	11.60
M3	1000-1400 µm	550 ^oC, 2hr, 10 C/min	25.9	850 ^oC, 1 hr CO_2	731	69.88	7.80
AC1	<590 µm	550 ^oC, 2hr, 10 C/min	25.5	700 ^oC, 1 hr CO_2	397	4.67	24.32
AC2	<590 µm	550 ^oC, 2hr,10 C/min	25.5	750 ^oC, 1 hr CO_2	524	17.73	20.98
AC3	<590 µm	550 ^oC, 2hr,10 C/min	25.5	800 ^oC, 1 hr CO_2	630	37.64	15.90
AC4	<590 µm	550 ^oC, 2hr,10 C/min	25.5	825 ^oC, 1 hr CO_2	750	43.14	14.50
AC5	<590 µm	550 ^oC, 2hr,10 C/min	25.5	850 ^oC,1 hr CO_2	525	67.59	8.27
AC6	<590 µm	550 ^oC, 2hr,10 C/min	25.5	900 ^oC,1 hr CO_2	367	82.35	4.67
CA	<590 µm	No carbonization	NA	550 ^oC, 2 hr N_2	895	45.31	NA
COM	NA	NA	NA	NA	NA	489	NA

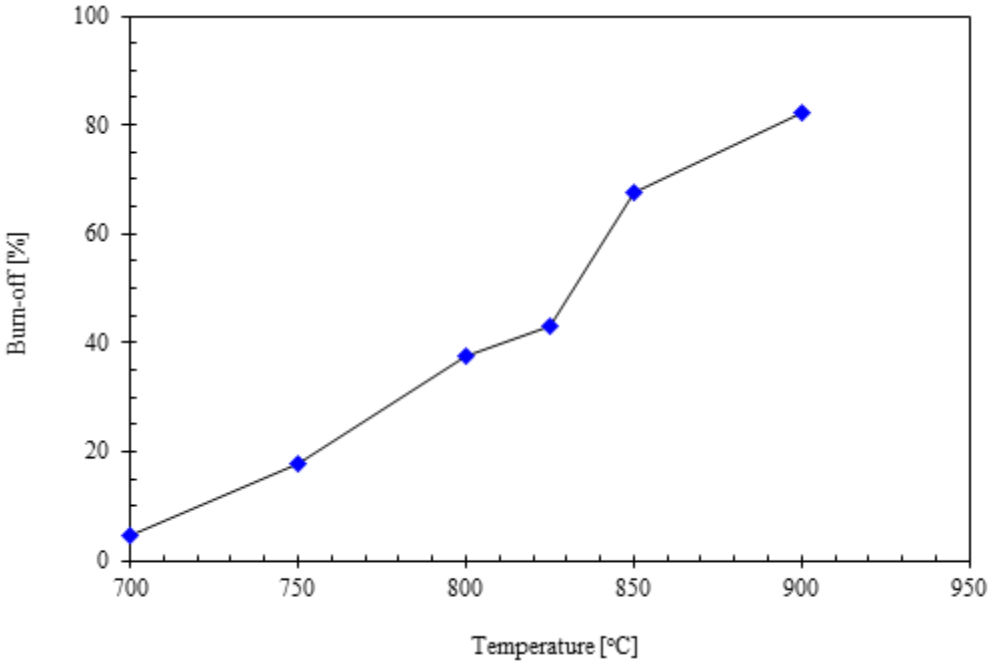

Figure 4.1 Burn-off of AC series versus activation temperature

BET surface area was also measured for all of the ACs shown in Table 4.4. Surface area is an important parameter in the adsorption process. For AC series, surface area is plotted versus the activation temperature in Figure 4.2. Interestingly, as the temperature increased, surface area also increased to a certain activation temperature. Further increase in temperature resulted in decline in surface area. The optimum activation temperature based on surface area was 825°C where the surface area was 750 m^2/g. The same trend can be seen in Figure 4.3 where N and M series surface area are plotted versus activation temperature. The optimum activation again was 825 °C, which N and M has 720 and 739 m^2/g respectively.

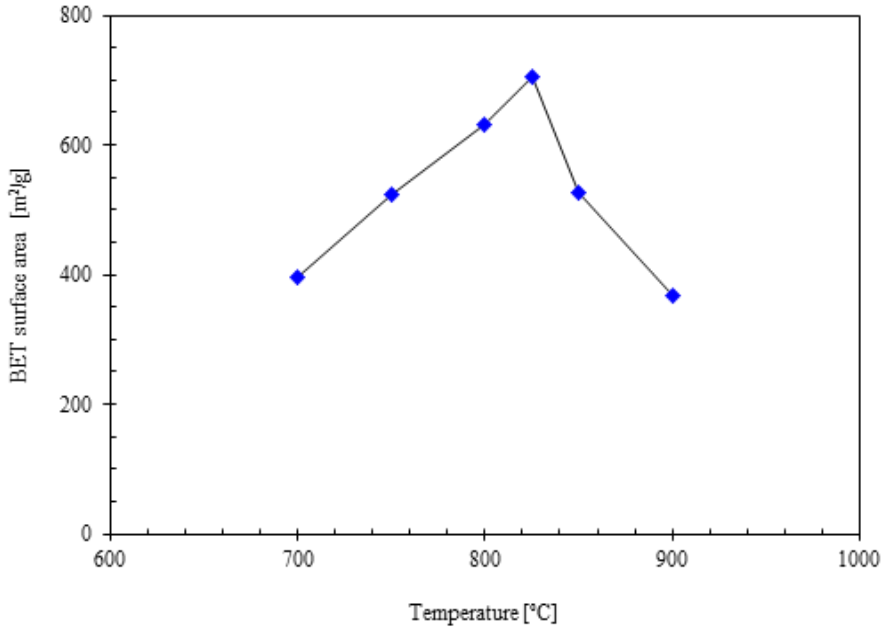

Figure 4.2 Surface area of AC series versus activation temperature

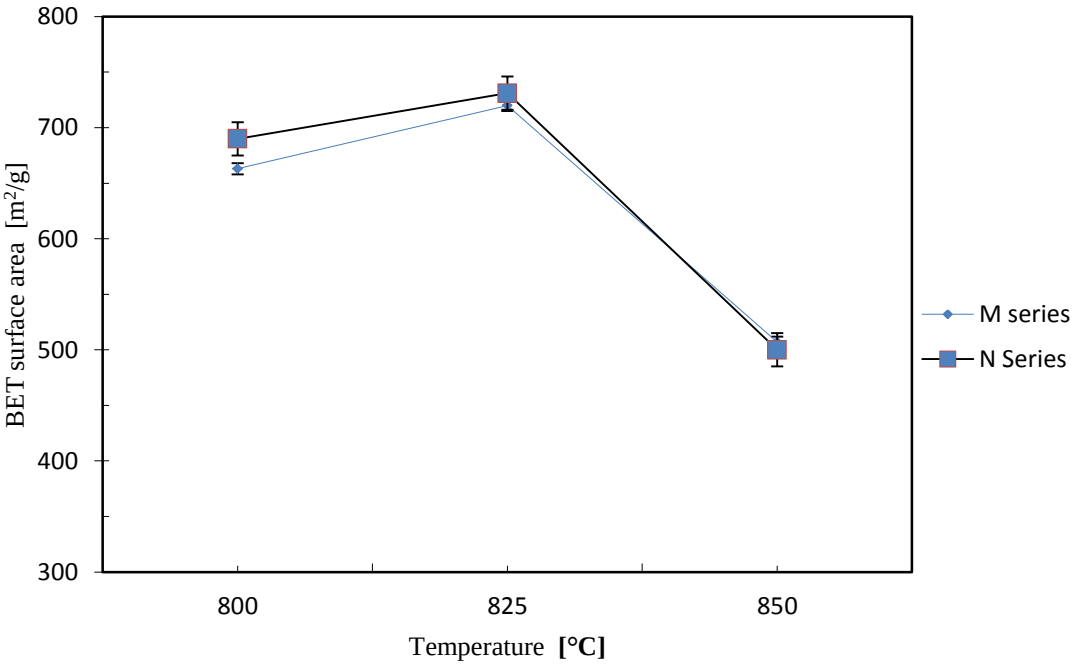

Figure 4.3 Surface area of N and M series versus activation temperature

The surface areas of the physically produced ACs were between 500 and 731 m^2/g. As the temperature increased, the surface area also increased to a point, after which the surface area decreased. The highest surface area of 731 m^2/g was for the M3 sample, which was produced at 825°C. Beyond 825°C, the surface area of the produced AC dramatically decreased. This can be attributed to an increasing percentage of ash in the AC. Ash is basically mineral material that is nonporous material. This trend was also seen in Lua and Guo (2000) who showed that produced AC at 950 °C activation temperature had lower surface area than at 850°C. They have stated that the C–CO_2 reaction was so severe at high temperature that it resulted in a high burn-off and was detrimental to the quality of ACs and surface area. Due to high extent of C-CO_2 reaction, biomass structure may be ruined, therefore surface area will decrease.

To develop a better understanding of produced AC, pore size distribution and micorposity needs to be analyzed. In Table 4.4, t-Plot Micropore Area, BJH desorption and t-Plot micropore volume are shown.

As can be seen in Table 4.4, physically ACs yielded mainly micropores while by comparison, chemically AC has more mesopore surface area. Microporosity may be the result of CO_2 activation. Having a greater surface area and greater mesopore size makes chemically AC favorable for adsorbing organics in water. Commercially AC which was provided on behalf of the Norit® company is considered to be useful for waste water treatment applications. Norit claimed that their AC has a surface area of 600 m^2/g but the measurements performed in the lab indicated a surface area of only 489 m^2/g.

Table 4.4 BET surface area and microporsity of activated carbons

Sample Name	BET Surface area	t-plot Micropore area(m^2/g)	t-plot micropore volume (cm^3/g)	Single point adsorption total pore volume of pores less than 8.087 Å width at p/p° = 0.034959495
N1	663.60	576.46	0.2800	NA
N2	731.65	618.87	0.2974	NA
N3	507.21	439.44	0.2706	NA
M1	690.61	586.23	0.2834	NA
M2	720.24	607.46	0.2944	NA
M3	501.35	422.45	0.2698	NA
Com	489.51	229.00	0.1133	NA
CA	895.23	613.01	0.2980	NA
AC1	396.55	392.36	0.1617	NA
AC2	524.47	467.67	0.2340	NA
AC3	632.36	619.52	0.2547	NA
AC4	705.27	596.68	0.2678	NA
AC5	525.78	487.66	0.2456	NA
AC6	365.14	308.57	0.19882	NA
B500	233.93	NA	NA	0.066590 cm^3/g
B1000	296.34	NA	NA	0.084886 cm^3/g
B1400	290.05	NA	NA	0.082902 cm^3/g

As can be observed in Table 4.4, the ACs have almost same surface area, mesopores and pore width regardless of particle size. The effect of temperature of production of AC can be analyzed in term of creating more surface area rather than changing pore width and widening the pore size.

In Figures 4.4 to 4.11 pore size volume versus pore width is shown for N1, N2, M1, M2, AC3, AC4, CA and Com respectively. By aid of these graphs, pore size distribution can be illustrated. It is notable that all physically ACs had almost the same trend in pore volume versus pore width which represents pore size distribution. As shown in the figures, there are two peaks in that curve. First peak is in the micro size range and the second peak is in the meso size range. Although physically ACs have two peaks, it seems that micropores dominate mesopores. Therefore the average shows in the micropre size range. The two-peak distribution can be attributed to CO_2 activation mechanism. In chemical activation most pore volume was of the micro size. In the commercial sample, there are several pore widths and probably most of pore volume is in the mesopore size range.

The effect of activation can be understood from the increase in surface area of biochar (prior to activation) and AC. For measuring BET surface area of biochar, CO_2 was used instead of N_2 so that micropores can be more readily detected than can be done using N_2. Attempts to use N_2 for measuring the BET surface area were largely a failure. Biochar showed the same BET surface area for all three samples. Biochar with mesh particle size of below 590 µm named B500. Biochars with particle size of 590-1000 µm and 1000-1400 µm named B1000 and B1400 respectively. B500, B1000 and B1400 went through activation and produced AC, M and N series respectively. In other word, they are precursor for production of ACs.

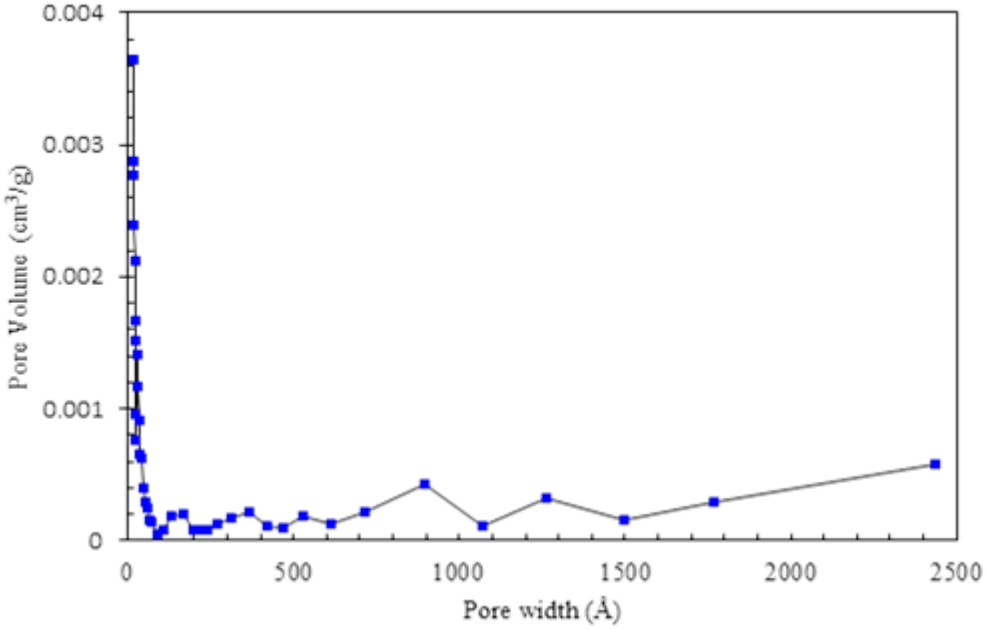

Figure 4.4 Pore volume versus pore width for N1

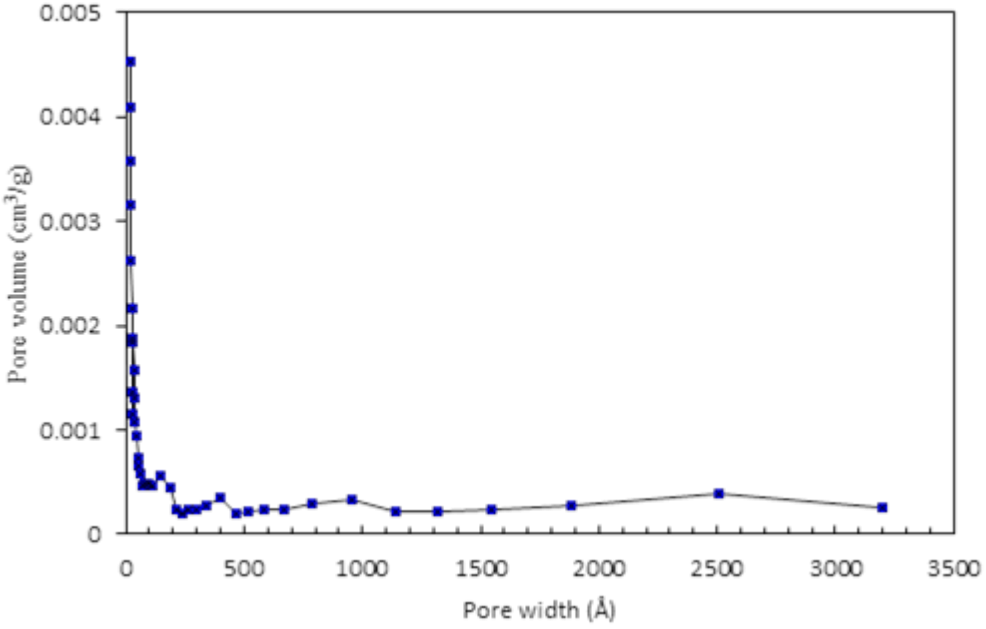

Figure 4.5 Pore volume versus pore width for N2

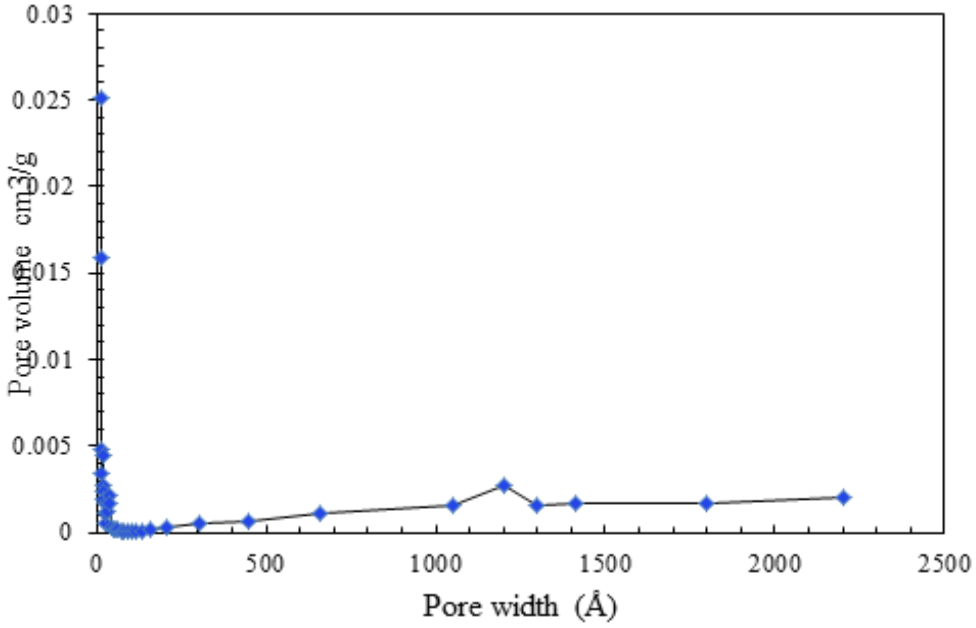

Figure 4.6 Pore volume versus pore width for M1

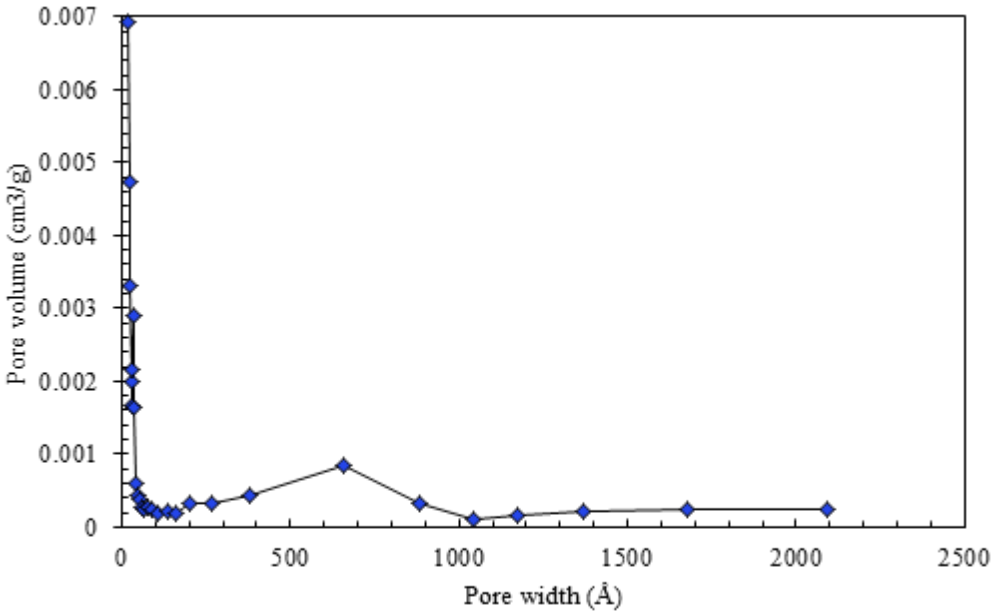

Figure 4.7 Pore volume versus pore width for M2

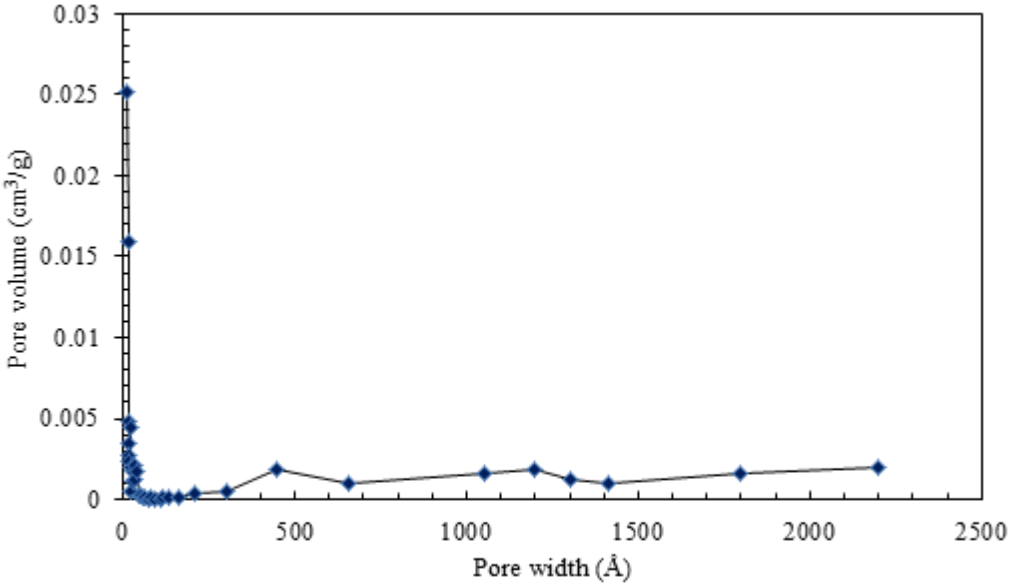

Figure 4.8 Pore volume versus pore width for AC3

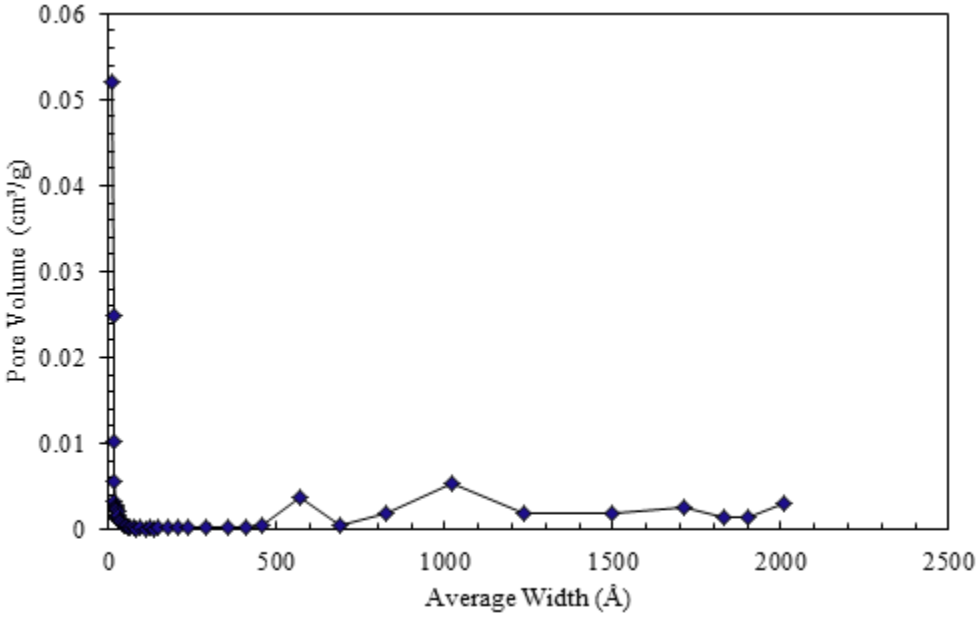

Figure 4.9 Pore volume versus pore width for AC4

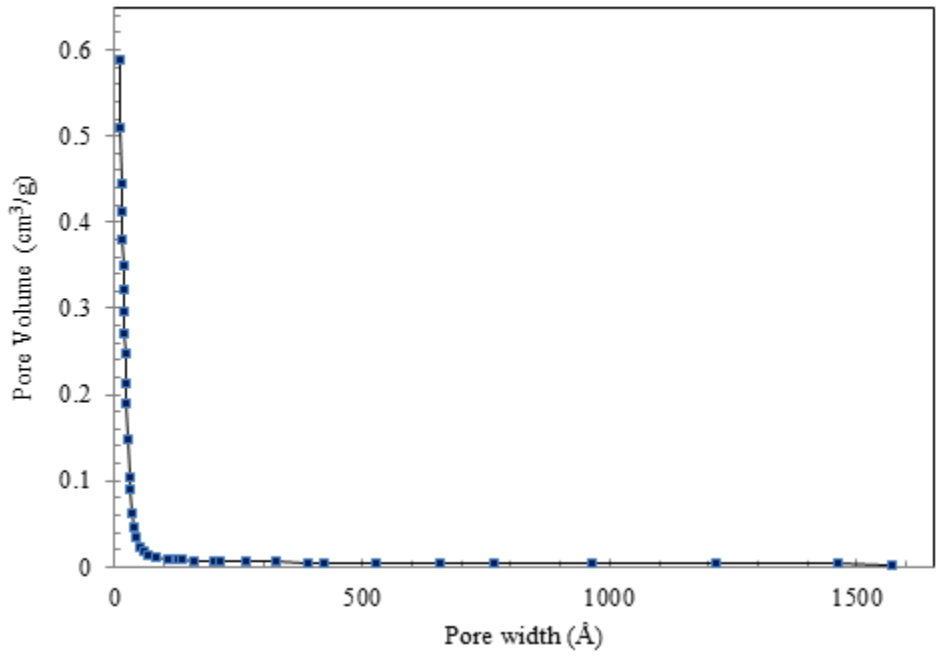

Figure 4.10 Pore volume versus pore width for CA

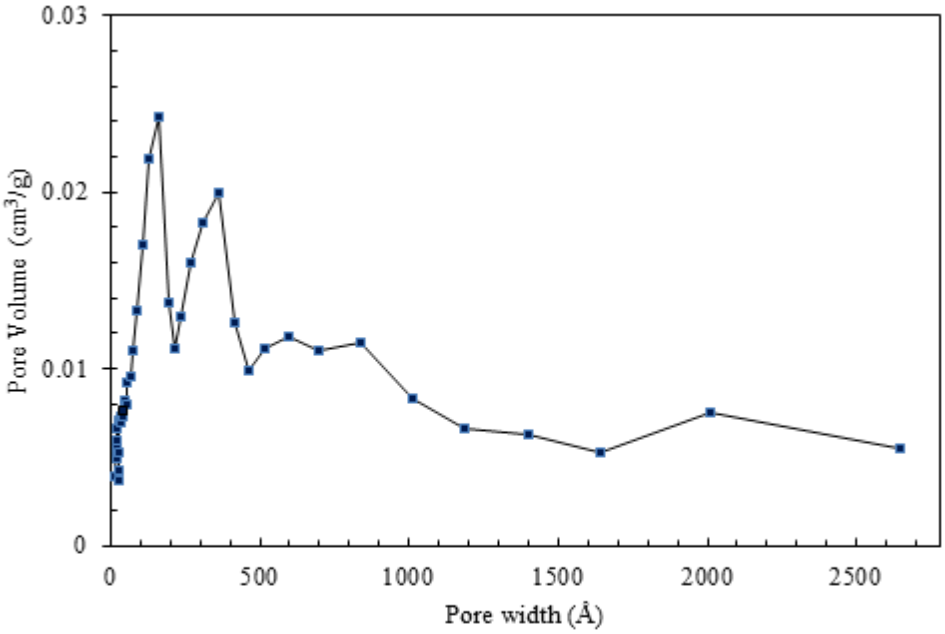

Figure 4.11 Pore volume versus pore width for Com

4.3 Elemental analysis, C, H, N and S

Elemental analysis was done to measure the C, H, N, and S content of the ACs and others samples are shown in Table 4.5. C content was between 64 to 88%, which was predictable based on initial biomass analysis because of the removal of humidity and volatiles. Chemically AC had the lowest C content among AC. The carbon content of commercial AC was around 64 percent.

Comparing C content of AC to biochar shows that C content decreased in the AC series. As temperature increased during activation, the C content decreased; which can be seen by comparing N1 with M2 and M1 with N2. An explanation for the decreasing C content of produced AC can be the reaction of C-CO_2 which leads to a decrease in carbon. The effect of activation temperature on the carbon content of AC is noticeable. Carbon content of the AC series is plotted versus their corresponding activation temperature in Figure 4.12. It seems that as activation temperature increases, carbon content of produced AC decreases. This trend can be seen in AC, N and M series. AC1 has richer carbon content than the rest of these series and it was close to biochar carbon content. The same trend can be observed for N and M series. N1 and M1 samples which both were produced at 800 °C, had richer carbon content than N2, M2, N3 and M3, which were produced at higher temperature.

Another interesting observation was the effect of particle size on the carbon content of AC. Activated carbon produced in the same activation temperature regardless of particle size had almost the same carbon content. This is the same effect as noticed in the case of the effect of particle size on BET surface area.

Table 4.5 Elemental analysis of produced activated carbon

Sample	Weigh (mg)	Carbon (%)	Hydrogen (%)	Nitrogen (%)	Sulfur (%)
CA	2.39	54.36	3.44	1.70	1.23
CA	2.19	54.13	3.36	1.80	1.32
Com	1.74	64.23	0.92	0.48	0.52
Com	1.91	64.03	1.02	0.51	0.58
AC1	2	84.75	0.04	1.17	1.03
AC1	2.07	85.91	0.03	0.77	1.33
AC2	1.86	80.35	0.75	1.26	1.15
AC2	1.98	81.64	0.77	1.28	1.19
AC3	1.461	75.20	2.00	2.09	1.21
AC3	1.44	74.32	1.84	2.03	1.11
AC4	2.05	70.34	2.03	1.86	1.90
AC4	1.61	71.81	1.96	1.98	1.67
AC5	1.54	69.31	2.35	1.95	1.23
AC5	2.00	68.48	2.45	1.78	1.21
AC6	1.23	63.43	2.76	1.92	1.73
AC6	1.42	62.93	2.53	1.89	1.52
N1	2.4	72.49	2.18	1.69	1.35
N1	1.58	73.47	1.94	1.58	1.02
N2	1.54	69.31	2.45	1.95	1.23
N2	2	68.48	2.45	1.78	1.21
N3	1.23	63.43	2.76	1.92	1.73
N3	1.42	62.93	2.53	1.89	1.52
M1	1.72	74.40	1.93	1.58	1.78
M1	1.57	73.85	1.83	1.70	1.86
M2	1.52	68.86	2.32	2.27	1.01
M2	1.25	67.46	2.32	2.04	1.28
M3	1.43	63.23	2.46	1.72	1. 23
M3	1.65	63.73	2.33	1.69	1.22
B500	1.24	83.45	1.87	2.24	0.45
B500	1.56	83.37	1.77	2.38	0.47

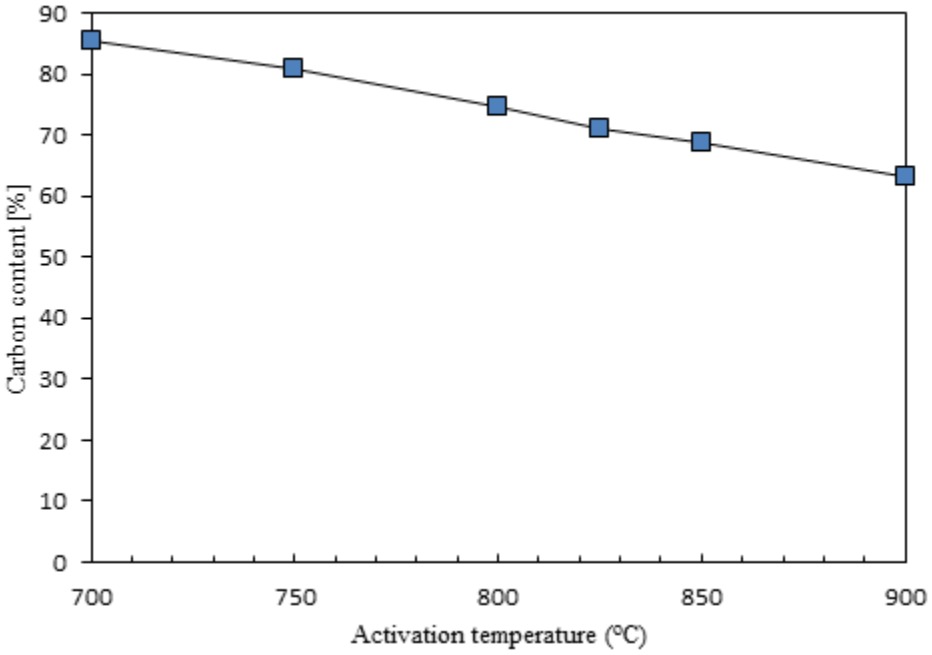

Figure 4.12 Carbon content of activated carbon versus their activation's temperature

4.4 TGA Results

TGA is used to compare the results in the reactor with a small chamber with precise measurements for physical activation. Samples undergo the same steps as biomass undergoes in the real reactor, such as heating ramp, final temperature and changing gas from N_2 to CO_2. The results, shown in Figures 4.13 – 4.16, indicate that the TGA data are consistent with the real results from the reactor. For each sample that underwent physical activation, two figures are shown: weight versus temperature and weight versus time. In addition to weight loss profile, the yield can be found from TGA data.

As the results show, the major weight loss happens at the beginning of the process where the carbonization occurs. Consistent with the literature, in these experiments the carbonization

step involves the production of a richer carbonaceous material and the removal of volatile material (Lehmann and Joseph, 2009). In the physical activation step there is not that much weight loss and trends were almost identical for all physically ACs.

Final yields calculated from TGA where very close to experimental data from the reactor. There was a small discrepancy that can be attributed to difference in heat transfer in the reactor and small TGA chamber. It is remarkable that yields from TGA were slightly lower than those from the real reactor, the main reason for that perhaps being the more uniform heat distribution provided in the TGA chamber therefore causing the reaction temperature to be higher.

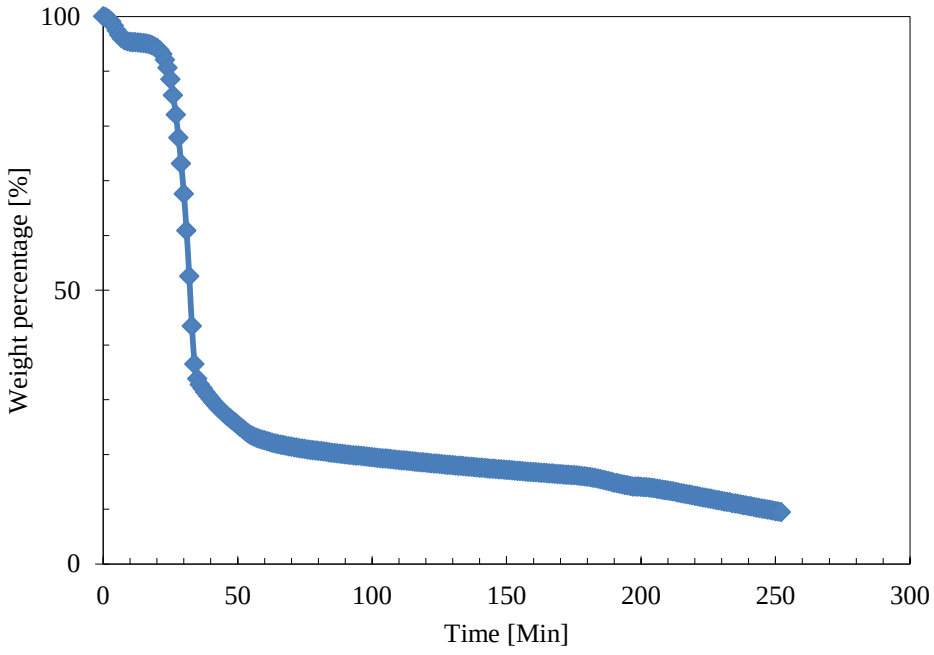

Figure 4.13 Weight loss of N1 versus Time

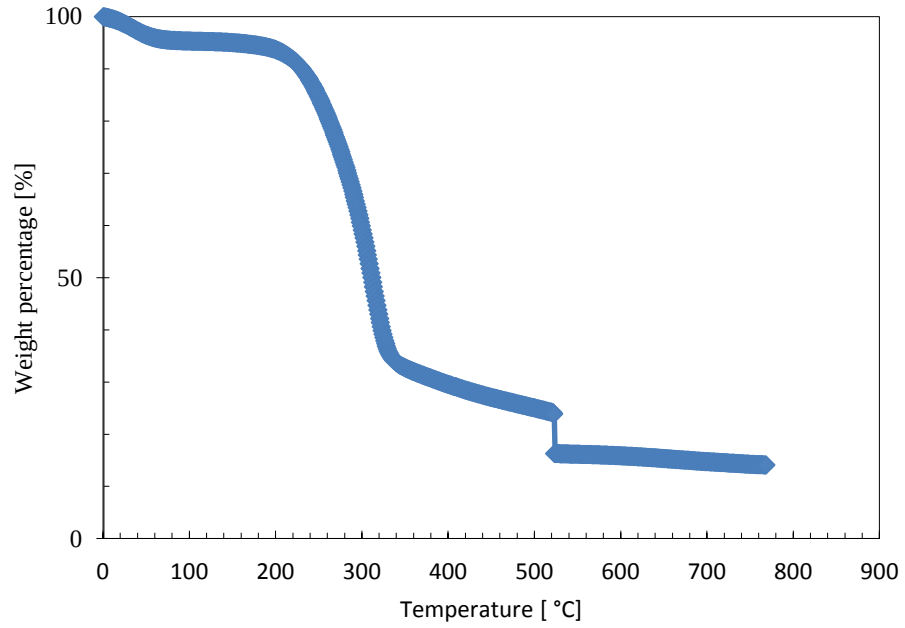

Figure 4.14 Weight loss of N1 versus Temperature

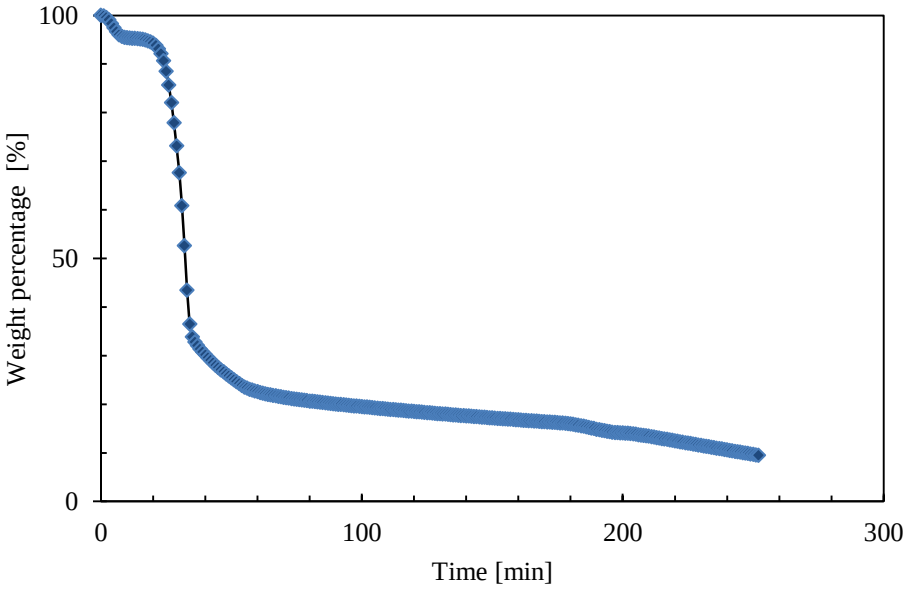

Figure 4.15 Weight loss of N2 versus Time

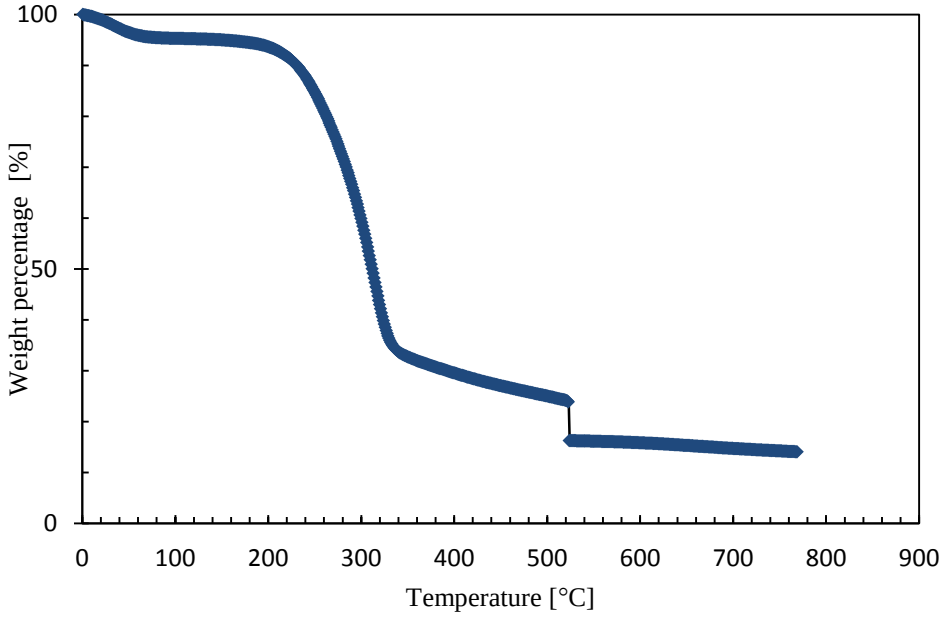

Figure 4.16 Weight loss of N2 versus Temperature

4.5 Synthetic Adsorption Tests

Adsorptions for each initial concentration of naphthenic acid are shown in the following Tables 4.6 – 4.10. N3 and M3 were not used for adsorption due to very low yields. In these tables the initial total carbon is shown as well as total organic carbon level after the adsorption. To calculate total organic carbon (TOC), inorganic carbon must be subtracted from total carbon. The initial concentrations were 18, 28.4, 32, 37 and 42 mg/l of TOC. The concentration was varied in order to investigate the performance of each AC at different concentration levels. Uptake percentage of physically AC was around 50-80%.

Among ACs, chemically activated carbon had the best adsorption uptake in comparison to the rest. The uptake percentage of the chemically activated carbon was around 80-90%. This

higher uptake ability could be due to higher surface area, more mesopore area or functional groups on AC.

M2 showed the best naphthenic acid uptake among the physically activated carbons. N1 showed similar performance to commercial AC. Activated carbon produced from mesh sized <590 µm showed an increase in TOC. This problem was tackled using different methods like decreasing pore size of nylon membrane from 1µm, 0.45 µm to 0.2 µm. Physically activated carbon caused an increase in inorganic carbon in the water, perhaps because of activation with CO_2.

An increase in inorganic carbon was observed through the use of physically activated carbon. The reason for that may be related to the usage of carbon dioxide for activation. Carbon dioxide may be attached on the surface of AC and then dissolved in the water creating bicarbonate and carbonate. Silica sand which was used as a standard, generally showed adsorption of 2 to 3 mg/l of NAs, while in Barnard's studies (2011) it was about 10 mg/l for the same amount of silica sand.

Biochar adsorption also showed increase TOC levels. This does not necessarily mean that no adsorption took place based on the definition of TOC. TOC refers to any organic material in the water; therefore it is not possible to distinguish NAs from any other organics. Biochar may leach out some volatiles in the water

Table 4.6 Adsorption results for activated carbon for initial point 18 mg/l

	TC (mg/l)	IC (mg/l)	TOC (mg/l)	uptake percentage (%)
Com	7.03	2.03	5	72
CA	3.5	0	3.5	91
N1	9.85	4.60	5.25	71
M2	7.5	3.43	4.07	77
M1	7.01	3.01	4.00	78
N2	9.05	6.00	3.05	83
AC3	20.56	4.25	16.31	
AC4	21.45	4.51	16.94	
B590	29.68	2.00	27.68	
B1000	26.34	2.35	23.99	
B1400	25.75	2.26	23.49	
Initial Point	18	0.00	18	0
Silica Sand	16	0.00	16	11

Table 4.7 Adsorption results for activated carbon for initial point 25.75 mg/l

	TC (mg/l)	IC (mg/l)	TOC (mg/l)	uptake percentage (%)
Com	12.88	1.88	11	61
CA	5.5	0	5.5	81
N1	12.97	3.97	9.00	68
M2	11.9	4.9	7.00	75
M1	10.26	4	6.26	78
N2	11.48	5.98	5.50	81
AC3	30.48	4.30	26.18	
AC4	32.01	4.51	27.5	
B500	34.50	2.01	32.49	
B590	32.14	2.35	29.79	
B1000	31.45	2.26	29.19	
Initial Point	28.4	0.00	28.4	0
Silica Sand	25.75	0.00	25.75	9

Table 4.8 Adsorption results for activated carbon for initial point 32 mg/l

	TC (mg/l)	IC (mg/l)	TOC (mg/l)	uptake percentage (%)
Com	14.6	1.6	13	59
CA	6.5	0	6.5	80
N1	14.85	2.87	11.98	63
M2	12.54	3.86	8.03	75
M1	11.43	3.4	8.03	75
N2	13	5.98	7.02	78
AC3	33.14	4.45	33.14	
AC4	35.04	4.71	30.33	
B5900	38.47	2.31	36.16	
B1000	36.24	2.80	33.44	
B1400	34.14	2.43	31.71	
Initial Point	32	0.00	32	0
Silica Sand	30	0.00	30	6

Table 4.9 Adsorption results for activated carbon for initial point 34 mg/l

	TC (mg/l)	IC (mg/l)	TOC (mg/l)	uptake percentage (%)
Com	18.6	1.6	17	54
CA	8	0	8	78
N1	16.5	3.11	13.39	64
M2	15.62	3.7	11.92	68
M1	14.15	3.8	10.35	72
N2	15.58	5.98	9.6	74
AC3	38.35	3.84	34.51	
AC4	39.25	3.45	35.8	
B590	42.41	2.01	40.4	
B1000	37.78	2.35	35.43	
B1400	36.68	2.26	34.42	
Initial Point	37	0.00	37	0
Silica Sand	34	0.00	34	8

Table 4.10 Adsorption results for activated carbon for initial point 42 mg/l

	TC (mg//l)	IC (mg/l)	TOC (mg/l)	uptake percentage (%)
Com	21.8	1.8	20	52
CA	10.5	0	10.5	75
N1	20.15	3.11	17.04	59
M2	17.17	3.187	13.983	67
M1	14.99	3.49	11.5	73
N2	16.15	4.15	12	71
AC3	43.20	3.25	39.95	
AC4	44.15	3.51	40.64	
B590	46.78	2.01	44.77	
B1000	43.64	2.35	41.29	
B1400	42.24	2.26	39.98	
Initial Point	42	0.00	42	0
Silica Sand	40	0.00	40	5

In order to investigate the leaching out of organics from biochar into the water, 3 biochar samples were placed in deionized water with the same conditions as the adsorption conditions. The TOC level was measured after 24 hours of shaking the samples. The results are shown in Table 4.11. The TOC level of the deionized water increased dramatically with the biochar samples. It seems that biochar leached out some organics, and the TOC increased to 10 mg/l in the water. In ACs with particle sizes bigger that 590 μm (M and N samples), the TOC remained

the same, but there was an increase in the inorganic carbon material, such as carbonate and bicarbonate that can come from CO_2 on the surface of AC.

Table 4.11 Biochar sample's TOC level in deionized water in the adsorption condition

Sample name	TC (mg/l)	IC (mg/l)	TOC (mg/l)
B590	19.34	1.32	18.02
B1000	12.75	1.82	10.93
B1400	13.23	1.73	11.50
AC3	9.23	3.32	5.91
AC4	8.32	2.92	5.40

For plotting the isotherm and comparing ACs in a wider range, the adsorption capacity, q, was used. The adsorption capacity can be defined by the following formula:

$$q = \frac{(C_0 - C_e)V}{W} \quad 4\text{-}1$$

where C_0 is (mg/l) the initial NA concentrations, C_e is the equilibrium concentration, V is the volume of the solution (l), and W is the mass of dry adsorbent used (g). The unit of q is mg of adsorbed NAs per 1 g of AC.

In order to investigate this effect the isotherm q should be plotted versus initial concentration. Apparently the chemically activated carbon CA sample had the best adsorption at all initial points. Commercially activated carbon had the lowest adsorption ability among ACs. To see the effect of initial concentration, q is plotted versus its initial concentration in Figure 4.17. Chemically activated carbon had better uptake at all initial points and next best performance was demonstrated by N2 and M1., with N2 having slightly better performance than M1 in NA adsorption. M2, N1 and commercially activated carbon ranked next.

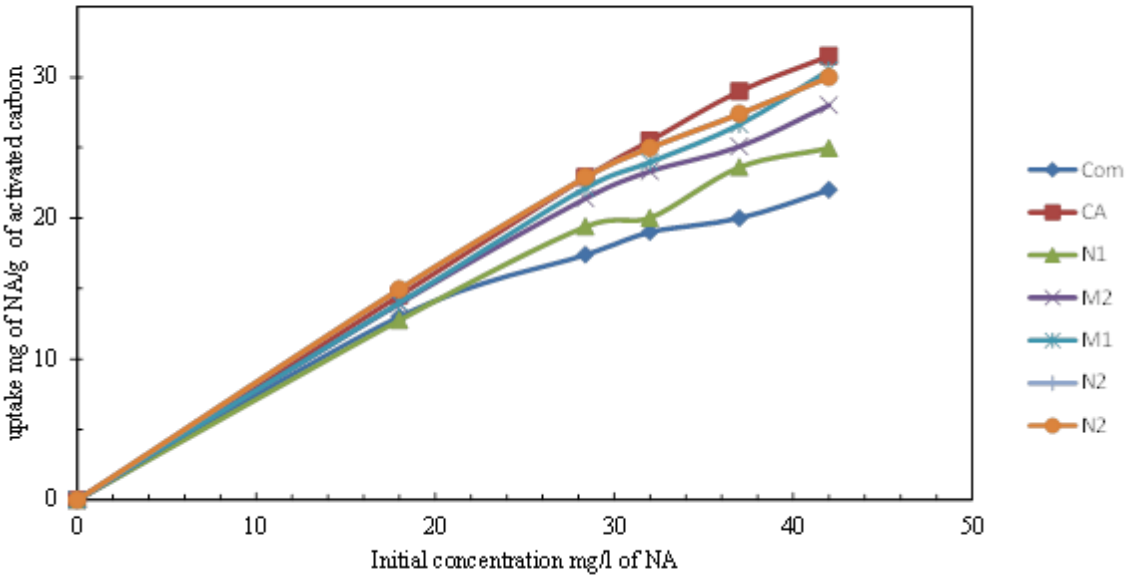

Figure 4.17 Uptake ability versus initial concentration for different activated carbons

Compared in terms of BET surface area, the samples rank in the following order: CA>N2>M1>M2>N1>Com. In terms of adsorption uptake, the ranking is: CA> N2 > M2>M1>N1>Com reflecting almost the same trend in adsorption ability as BET surface area.

4.6 Isotherm Data and Modeling

Isotherm data for N1, N2, M1, M2, CA, Com is shown in Figure 4.18 – 4.23, where q versus equilibrium concentration Ce is depicted for all ACs used in adsorption tests. Langmuir, Freundlich and Sips isotherms were used for the modeling of experimental data. R^2 represents correlation coefficient.

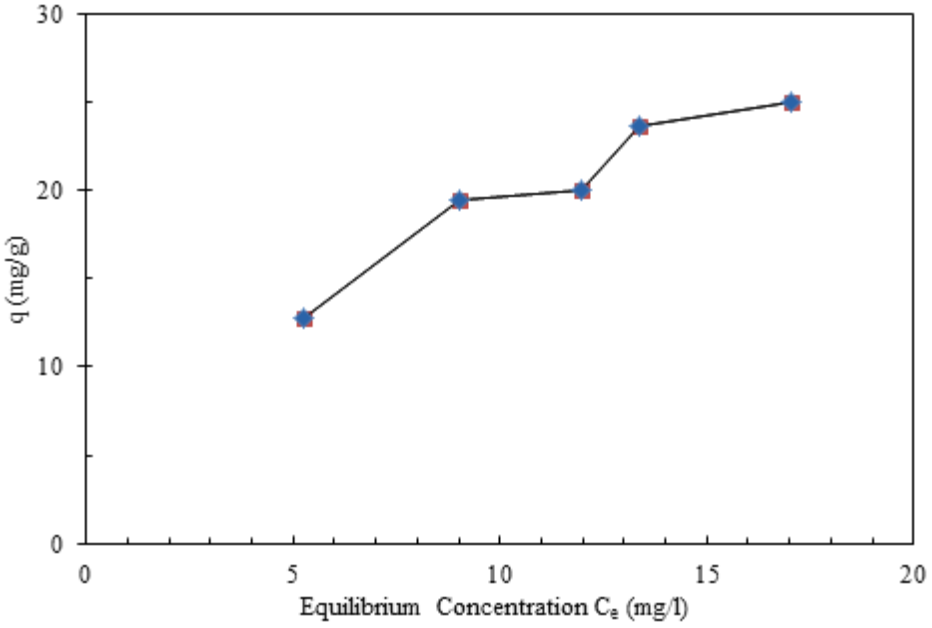

Figure 4.18 Isotherm data for N1

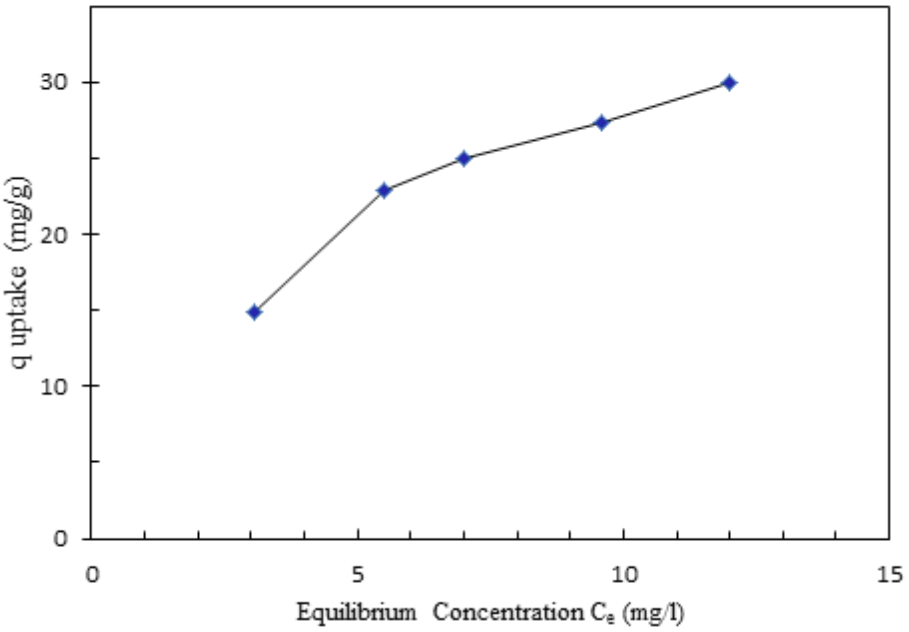

Figure 4.19 Isotherm data for N2

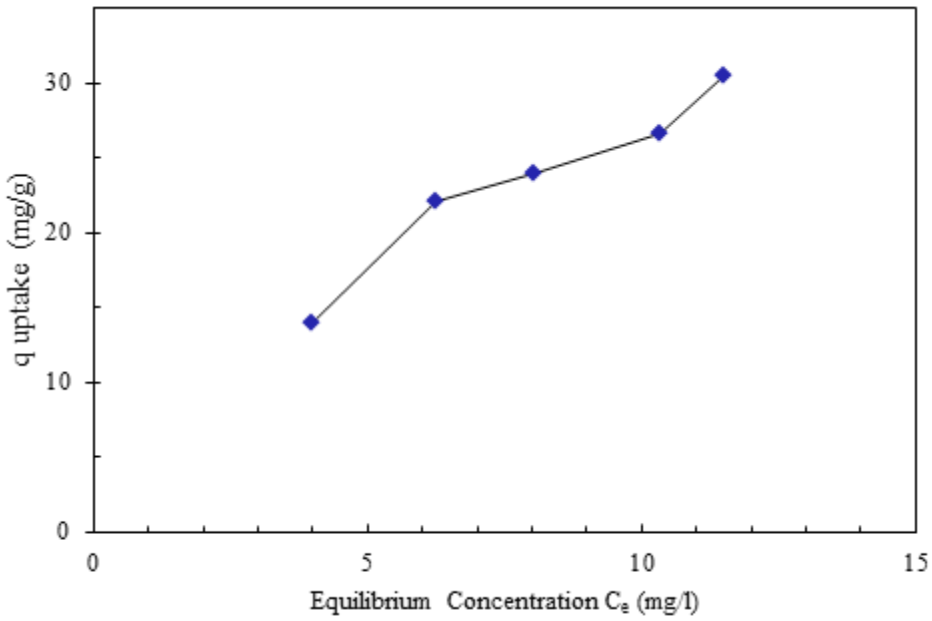

Figure 4.20 Isotherm data for M1

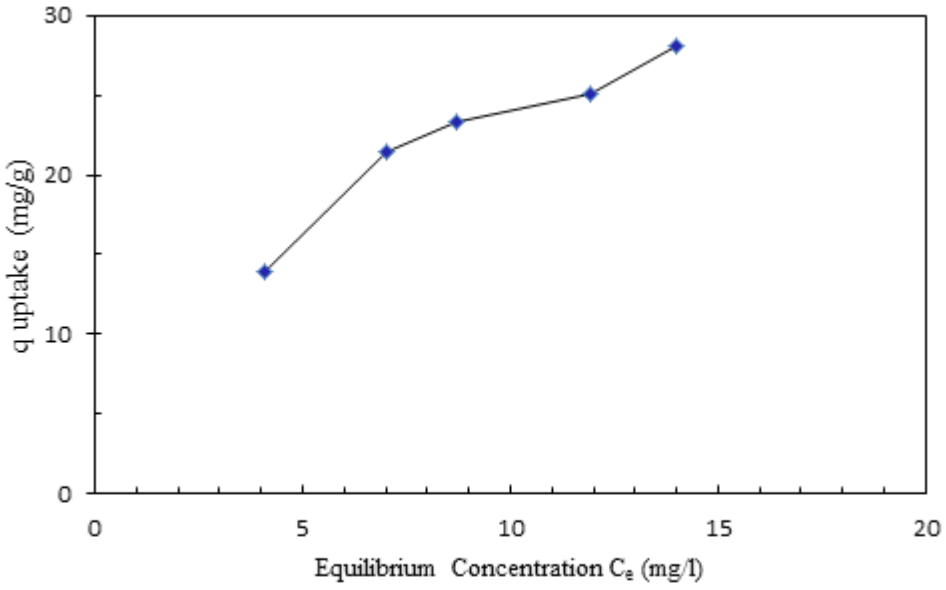

Figure 4.21 Isotherm data for M2

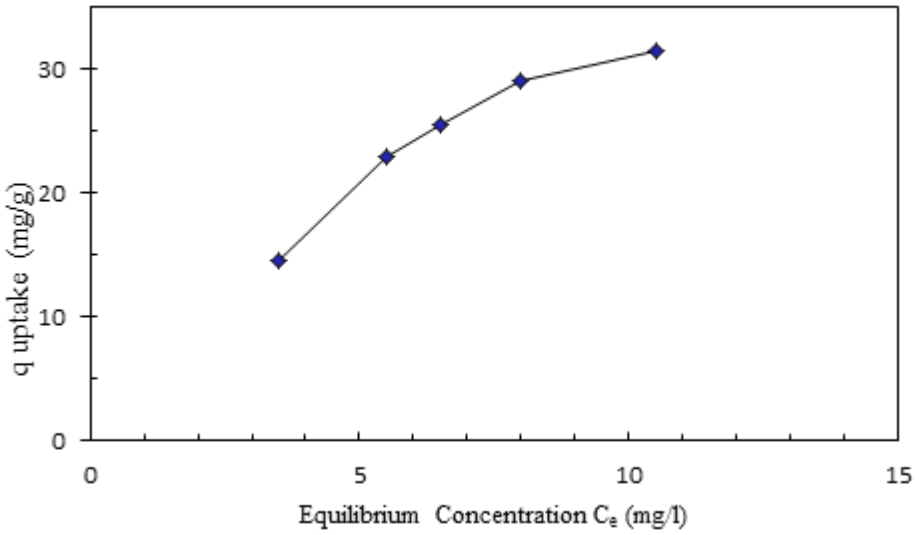

Figure 4.22 Isotherm data for CA

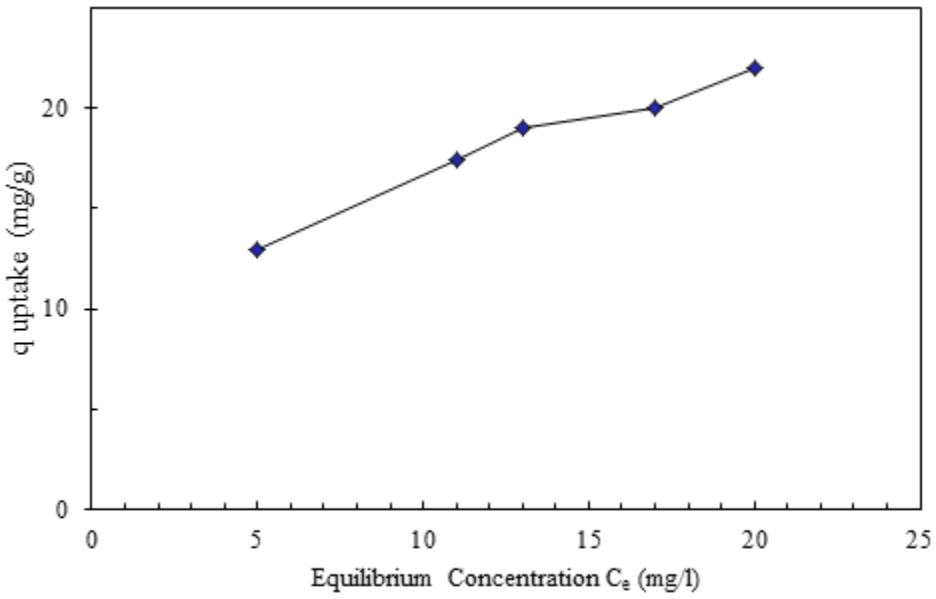

Figure 4.23 Isotherm data for Com

Fitting parameters for modelling are shown in Table 4.12. The constants for equations in Table 4.12 are described in equations 2.2, 2.3 and 2.5. For physically activated carbon generally the Langmuir isotherm showed a better fit than Freundlich. Because the best fit was Langmuir, it indicates that adsorption was monolayer on the AC. Generally Sips isotherm showed a better R^2, attributed to this model having three fitting parameters.

One of the produced activated carbons, M1, which was the best sample in this study, was provided to Kimetu et al. (2012) to investigate the ability of removal of organics from Industrial SAGD water. The initial TOC level of the industrial water was 656.5 mg/l and pH of water was 9.8. For the purposes of this study samples from several different sources including over twenty corporate entities and institutions across North America, were collected and compiled together creating a broader sample base. The adsorption condition was at 80 °C to simulate the real temperature in the SAGD operation. The TOC content of the water after this treatment by M1 activated carbon dropped to 319.1±10.4 from 656.5±3.2. The performance of M1 was outstanding comparing to the other biochars (Kimetu et al. 2012).

Table 4.12 Modelling data for produced activated carbon

	Freundlich			Langmuir			Sips			
	K	n	R^2	q_m	B	R^2	q_m	B	n	R^2
CA	7.473	1.5832	0.9239	66.75	0.09069	0.968	36.49	0.2336	0.4801	0.998
Com	7.200	2.7056	0.9892	27.64	0.1683	0.9751	123.6	0.001371	2.3283	0.9893
M1	6.277	1.5625	0.9532	62.72	0.07803	0.9611	39.92	0.1707	0.6649	0.9651
M2	7.658	2.0247	0.9476	43.33	0.1274	0.9717	31.69	0.2143	0.6053	0.9829
N1	5.912	1.4388	0.9856	100.8	0.0418	0.9877	110.4	0.03533	1.039	0.9877
N2	9.914	2.2011	0.9573	43.61	0.185	0.9863	34.66	0.2747	0.6761	0.9943

Chapter Five: **Conclusions and Recommendations**

5.1 Conclusions

In this work it has been shown that activated carbon produced from wood waste (sawdust) was effective for the removal of organic compounds from aqueous solutions by adsorption and that the activated biochar performed better than a commercially-produced AC. A removal range between 60-90% of total organic carbon (TOC) was achieved using ACs produced in this study for different concentrations of contaminants. The water treated contained TOC resulting mainly from the presence of naphthenic acids.

In biochar production, the carbonization temperature showed the strongest effect on yield of produced biochars. Heating rate and activation time were ranked 2nd and 3rd respectively. Generally a yield of around 20-30% is expected during the production of biochar from sawdust. The biochar production condition employed prior to activation remained constant for production of AC: the temperature condition for production of biochar before activation was 550°C with a heating ramp rate of 10°C/min and samples were kept 2 hours in the reactor. The surface areas for the produced biochars with particle size of below 590 µm, 590-1000 µm and 1000-1400 µm were 233.93, 296.34 and 290.05 m^2/g respectively.

After the production of biochar, physical activation was studied. Among the physical production conditions, activation temperature was shown to be the most important because of its effect on the carbon content and the burn-off. Activation temperature enhanced the extent of the reactions evidenced by decreasing carbon content and increasing rate of burn-off. Increasing activation temperature and increased surface area of AC created an optimum temperature which once surpassed led to the surface area deceasing as the temperature

increased. This optimum temperature was determined to be 825°C. As the surface area increased, the adsorption capacity increased.

The decrease of surface area at higher temperature 825°C can be attributed to an extensive C-CO_2 reaction and increasing the ash content in the AC. It was found that particle size of the biomass feedstock did not have a significant effect on the surface area and adsorption characteristics of the produced AC. All produced ACs, despite their production conditions, displayed similar trends of microprosity and mesoprosity. The pore size distributions in physical activation had two peaks, one peak obtained in microprosity area and the other one in the mesoprosity. Although chemically activated carbon had more surface area and more mesopores, its adsorption capacity was close to that of physically activated carbon. In the adsorption tests for the majority of adsorbents, TOC levels were decreased due to adsorption on AC. As a baseline, the resulting TOC level following filtration using AC was compared to removal of TOC by filtration through silica sand. Among the materials used for adsorption, an increase in TOC was observed in biochar samples and physically activated carbon with particle size below 590 μm. This increase was shown to be attributed to the leaching out of organics in the biochars and passing of fine carbon particles through the filter. Among the ACs, chemically activated carbon showed the lowest tendency to donate organics to the water.

Langmuir, Freundlich and Sip isotherms were used for modeling the experimental results. Langmuir isotherm fit the best for the experimental data. Therefore, it may be concluded that the adsorption is a monolayer model for physical activation. For chemically activated carbon and commercial activated carbon, Sip isotherm and Freundlich were the best respectively.

If we assume that Alberta oil sands mining provides 848,000 barrel of equivalent oil (boe)/day and 2 barrels of water ends up in tailings ponds per boe produced, then each year 73.81 million m^3 of water must be treated (Alberta Energy, 2012). Assuming that NA is present in the water at 58 mg C/L and that 80% of the NA must be removed to meet a suitable standard, each year 4300 tC would need to be removed from the tailings water. Given the activated carbon developed here can remove 25 mg C NA carbon per g activated carbon, 14,300 t activated carbon would be needed to used to treat the annual production of water from tailings operations. To produce this activated carbon, assuming a yield of only 13-18%, would require 0.95 to 1.32 Mt dry biomass. To put this into perspective, the annual forest roundwood production in Alberta is 22 Mm^3/year, or about 11 Mt dry biomass by assuming 0.5 t dry/m3 roundwood (Canadian Council of Forest Ministers, 2010).

5.2 Recommendations

Physical activation of biochar produced from sawdust showed a low yield. As discussed, the low yield may mostly due to the low carbon content of sawdust. Therefore, using a precursor biomass with higher carbon content may improve on this situation. For developing further understanding of the nature and properties of AC more tests can be done. FTIR and SEM can be very useful for investigation of features such as the nature and structure of the functional groups in the ACs. The effect of various process parameters on the characteristics of the ACs produced from physical activation can be further investigated. The flow rates of activation agent, residence time are crucial to final AC character and can be evaluated further with additional tests.

A possible solution for removal of organics in tailings ponds can be using column adsorption units. It is expected that the performance of AC in packed columns will be different

than the performance in batch operations. In batch tests, thermodynamics of adsorption is the key factor while in column tests both kinetics and thermodynamics will be important. Thus batch tests would not guarantee an acceptable performance. Column tests are recommended for further study of the performance of produced AC.

Given the complexity of the problem of removal of naphthenic acid from tailing ponds, a commercial grade of naphthenic acid in a deionized solution was used this studied. For more representative results, greater use of actual tailings pond water samples is recommended for future studies. In an actual sample, multi-adsorption phenomena will take place because of the variety of organic compounds present and it is expected that each compound will be adsorbed differently and will interfere with the adsorption of other species present in the water. TOC measurements are unable to distinguish between the naphthenic acid and other organic compounds present in water samples. Therefore, TOC measurement, which was used in this study, will not be sufficient to distinguish the different adsorption characteristics among the various organic species in actual tailings and produced water samples and more sophisticated analyses will be required. FTIR or GC-MS techniques will be useful for more detailed differentiation of adsorption characteristics of various organic species in the water.

References

Adinata, D., W. Daud and M. Aroua (2007). "Preparation and characterization of activated carbon from palm shell by chemical activation with K2CO3." Bioresource Technology 98(1): 145.

Alberta Energy (2012). Facts and Statistics, http://www.energy.alberta.ca/oilsands/791.asp, retrieved Dec.2012

Alberta Environment (2012). Oil Sands Opportunity Balance, http://www.environment.alberta.ca/documents/oil_sands_opportunity_balance.pdf, retrieved Nov.2012

Alberta Geological Survey (2012) http://articles.businessinsider.com/2012-04-24/news/31391071_1_oil-sands-tar-sands-crude-oil

Allen, E., (2008). A. "Process water treatment in Canada's oil sands industry: I. Target pollutants and treatment objectives." Journal of Environmental Engineering and Science 7(2): 123-138.

Allen, E. (2008). B. "Process water treatment in Canada's oil sands industry: II. A review of emerging technologies." Journal of Environmental Engineering and Science 7(5): 499-524.

Aravindhan, R., J. Rao and B. U. Nair (2009). "Preparation and characterization of activated carbon from marine macro-algal biomass." Journal of Hazardous Materials 162(2-3): 688.

Aroua, M., S. Leong, L. Y. Teo, C. Yin and W. Daud (2008). "Real-time determination of kinetics of adsorption of lead(II) onto palm shell-based activated carbon using ion selective electrode." Bioresource Technology 99(13): 5786.

Aworn, A., P. Thiravetyan and W. Nakbanpote (2009). "Preparation of CO2 activated carbon from corncob for monoethylene glycol adsorption." Colloids and Surfaces A: Physicochemical and Engineering Aspects 333(1-3): 19.

Azargohar, R. and A. Dalai (2008). "Steam and KOH activation of biochar: Experimental and modeling studies." Microporous and Mesoporous Materials 110(2-3): 413.

Bagheri, N. and J. Abedi (2009). "Preparation of high surface area activated carbonAC from corn by chemical activation using potassium hydroxide." Chemical Engineering Research and Design 87(8): 1059.

Bansal, R., (2005). Activated Carbon Adsorption., London,CRC Press. ISBN: 0824753445

Barnard, Z. (2011). Conversion of Petroleum Coke to Activated Carbon and its application to Naphthenic Acid Removal from Tailings Pond Water. Master Thiese University of Calgary.

Benadjemia, M., L. Reinert, N. Benderdouche and L. Duclaux (2011) "Preparation, characterization and Methylene Blue adsorption of phosphoric acid activated carbons from globe artichoke leaves." Fuel Processing Technology 92(6): 1203.

Brient, J., P. Doyle, (2000). Kirk-Othmer Encyclopedia of Chemical Technology. New York, Wiley & Sons, Inc., ISBN: 0471484962

Canadian Council of Forest Ministers, 2010, National forestry database, http://nfdp.ccfm.org/products/quick_facts_e.php, retrieved Jan. 2013

Chang, C., C. Chang and W. Tsai (2000). "Effects of Burn-off and Activation Temperature on Preparation of Activated Carbon from Corn Cob Agrowaste by CO2 and Steam." Journal of Colloid and Interface Science 232(1): 45.

Choy, K., J. Barford and G. McKay (2005). "Production of activated carbon from bamboo scaffolding waste-process design, evaluation and sensitivity analysis." Chemical Engineering Journal 109(1-3): 147.

Clemente, J. and P. Fedorak (2005). "A review of the occurrence, analyses, toxicity, and biodegradation of naphthenic acids." Chemosphere 60(5): 585-600.

Daud, W., W. Ali and M. Sulaiman (2000). "The effects of carbonization temperature on pore development in palm-shell-based activated carbon." Carbon 38(14): 1925.

Deriszadeh, A. (2009). Improved MEUF treatment of produced water utilizing naphthenic acid co-contaminants. PhD, University of Calgary.

DiPanfilo, R. and N. Egiebor (1996). "Activated carbon production from synthetic crude coke." Fuel Processing Technology 46(3): 157.

Do, D. (1998). Adsorption analysis: Equilibria and kinetics. London, Imperial College Press. ISBN: 1860941370

Drzewicz, P., A. Afzal, M. El-Din and J. Martin (2010). "Degradation of a Model Naphthenic Acid, Cyclohexanoic Acid, by Vacuum UV (172 nm) and UV (254 nm)/H2O2." The Journal of Physical Chemistry A 114(45): 12067-12074.

Fukuyama, H. and S. Terai (2008). "Preparing and characterizing the active carbon produced by steam and carbon dioxide as a heavy oil hydrocracking catalyst support." Catalysis Today 130(2-4): 382.

Gaikar, V. and D. Maiti (1996). "Adsorptive recovery of naphthenic acids using ion-exchange resins." Reactive and Functional Polymers 31(2): 155-164.

Gamal El-Din, M., H. Fu, N. Wang, P. Chelme-Ayala, P. Drzewicz, J. W. Martin, Z. and D. Smith (2011) "Naphthenic acids speciation and removal during petroleum-coke adsorption and ozonation of oil sands process-affected water." Science of The Total Environment 409(23): 5119.

Gergova, K. and S. Eser (1996). "Effects of activation method on the pore structure of activated carbons from apricot stones." Carbon 34(7): 879.

Girgis, B. and A. El-Hendawy (2002). "Porosity development in activated carbons obtained from date pits under chemical activation with phosphoric acid." Microporous and Mesoporous Materials 52(2): 105.

Girods, P., A. Dufour, V. Fierro, Y. Rogaume, C. Rogaume, A. Zoulalian and A. Celzard (2009). "Activated carbons prepared from wood particleboard wastes: Characterisation and phenol adsorption capacities." Journal of Hazardous Materials 166(1): 491.

Guo, J. and A. Lua (2003a). "Surface Functional Groups on Oil-Palm-Shell Adsorbents Prepared by H3PO4 and KOH Activation and their Effects on Adsorptive Capacity." Chemical Engineering Research and Design 81(5): 585.

Guo, J. and A. Lua (2003b). "Textural and chemical properties of adsorbent prepared from palm shell by phosphoric acid activation." Materials Chemistry and Physics 80(1): 114.

Guo, J., W. Xu, Y. Chen and A. Lua (2005). "Adsorption of NH3 onto activated carbon prepared from palm shells impregnated with H2SO4." Journal of Colloid and Interface Science 281(2): 285.

Hayashi, J., Kazehaya, A., Muroyama, K. and Watkinson, A. (2000). "Preparation of activated carbon from lignin by chemical activation." Carbon 38(13): 1873-1878.

Holowenko, F., MacKinnon, M. and Fedorak, P. (2000). "Methanogens and sulfate-reducing bacteria in oil sands fine tailings waste." Canadian Journal of Microbiology 46(10): 927.

Holowenko, F. M., MacKinnon M. D. and Fedorak P. M. (2002). "Characterization of naphthenic acids in oil sands wastewaters by gas chromatography-mass spectrometry." Water Research 36(11): 2843.

Ip, A., J. Barford and G. McKay (2008). "Production and comparison of high surface area bamboo derived active carbons." Bioresource Technology 99(18): 8909.

Jia, L., E. J. Anthony, and J. P. Charland (2002). "Investigation of vanadium compounds in ashes from a CFBC firing 100% petroleum coke." Energy & Fuels 16(2): 397

Jia, Q. and A. Lua (2008). "Effects of pyrolysis conditions on the physical characteristics of oil-palm-shell activated carbons used in aqueous phase phenol adsorption." Journal of Analytical and Applied Pyrolysis 83(2): 175.

Johns, M., W. Marshall and C. Toles (1999). "The effect of activation method on the properties of pecan shell-activated carbons." Journal of Chemical Technology & Biotechnology 74(11): 1037.

Kimetu, J., D.,Layzell, J., Hill, M., Husein, J. Bergerson, 2012, Personal communication.

Laine, J., A. Calafat and M. labady (1989). "Preparation and characterization of activated carbons from coconut shell impregnated with phosphoric acid." Carbon 27(2): 191.

Lee, W. and Choi, "Preparation and characterization of activated carbons from corn cob." Carbon 21(1)- 181

Lehmann, J., Joseph S. (2009). Biochar for Environmental Management: Science and Technology. London, Earthscan. ISBN: 9781844076581

Lehr, J. (2005). Treatment of spent refinery caustic U. S. Patenet. U.S., Star Enterprise 5,434,329.

Lim, W., C. Srinivasakannan and N. Balasubramanian (2010). "Activation of palm shells by phosphoric acid impregnation for high yielding activated carbon." Journal of Analytical and Applied Pyrolysis 88(2): 181.

Lua, A. and J. Guo (2000). "Activated carbon prepared from oil palm stone by one-step CO2 activation for gaseous pollutant removal." Carbon 38(7): 1089.

Lua, A. and J. Guo (2001). "Microporous Oil-Palm-Shell Activated Carbon Prepared by Physical Activation for Gas-Phase Adsorption." Langmuir 17(22): 7112.

Lua, A. and Q. Jia (2009). "Adsorption of phenol by oil–palm-shell activated carbons in a fixed bed." Chemical Engineering Journal 150(2–3): 455-461.

Lua, A., T. Yang and J. Guo (2004). "Effects of pyrolysis conditions on the properties of activated carbons prepared from pistachio-nut shells." Journal of Analytical and Applied Pyrolysis 72(2): 279-287.

Maciria-Agullria, J., B. Moore, D. Cazorla-Amoras and A. Linares-Solano (2004). "Activation of coal tar pitch carbon fibres: Physical activation vs. chemical activation." Carbon 42(7): 1367.

MacKinnon, M., and Sethi, A. (1993). A comparison of physical and chemical properties of the tailing ponds at the Syncrude and Suncor oil sands plants. Our Petroleum Future Conference, Edmonton.

Nabais, J., P. Nunes, P. Carrott, M. Ribeiro Carrott, A. García and M. Díaz-Díez (2008). "Production of activated carbons from coffee endocarp by CO2 and steam activation." Fuel Processing Technology 89(3): 262-268.

Ng, C., W. Marshall, R. Rao, R. Bansode and J. Losso (2003). "Activated carbon from pecan shell: process description and economic analysis." Industrial Crops and Products 17(3): 209.

Ozçimen, D. and Y. Ersoy-Mericboyu, (2010). "Characterization of biochar and bio-oil samples obtained from carbonization of various biomass materials." Renewable Energy 35(9): 1319.

Ozçimen, D. and A. Ersoy-Meriçboyu (2008). "A study on the carbonization of grapeseed and chestnut shell." Fuel Processing Technology 89(11): 1041.

Perrich, J. (1981). Activated carbon adsorption for wastewater treatment., London ,CRC Press. ISBN: 0849356938

Rodríguez-Mirasol, J., T. Cordero and J. Rodríguez (1993). "Preparation and characterization of activated carbons from eucalyptus kraft lignin." Carbon 31(1): 87.

Rodríguez-Reinoso, F. and M. Molina-Sabio (1992). "Activated carbons from lignocellulosic materials by chemical and/or physical activation: an overview." Carbon 30(7): 1111.

Rogers, V., M. Wickstrom, K. Liber and M. MacKinnon (2002). "Acute and Subchronic Mammalian Toxicity of Naphthenic Acids from Oil Sands Tailings." Toxicological Sciences 66(2): 347-355.

Salehi, E., J. Abedi and T. Harding (2011). "Bio-oil from Sawdust: Effect of Operating Parameters on the Yield and Quality of Pyrolysis Products." Energy & Fuels 25(9): 4145-4154.

Salehi E., (2011). The Production of Bio-oil and Hydrogen from Biomass. Ph.D Thesis, University of Calgary.

Siddique T., R. Gupta, P. M. Fedorak, M. D. MacKinnon, J. M. Foght (2008). "A first approximation kinetic model to predict methane generation from an oil sands tailings settling basin." Chemosphere 72(2): 1573

Small, C. (2011). Activation of Delayed and Fluid Petroleum Coke for the Adsorption and Removal of Naphthenic Acids from Oil Sands Tailings Pond Water. M.Sc University of Alberta.

Sricharoenchaikul, V., C. Pechyen, D. Aht-ong and D. Atong (2007). "Preparation and Characterization of AC from the Pyrolysis of Physic Nut (Jatropha curcas L.) Waste." Energy & Fuels 22(1): 31-37.

Stavropoulos, G. and A. Zabaniotou (2009). "Minimizing ACs production cost." Fuel Processing Technology 90(7–8): 952-957.

Tan, I., A. Ahmad and B. Hameed (2008). "Adsorption of basic dye using AC prepared from oil palm shell: batch and fixed bed studies." Desalination 225(3): 13.

Teng, H., J. Ho, Y. Hsu and C. Hsieh (1996). "Preparation of ACs from Bituminous Coals with CO2 Activation. 1. Effects of Oxygen Content in Raw Coals." Industrial & Engineering Chemistry Research 35(11): 4043-4049.

Teng, H. and H. Lin (1998). "Activated carbon production from low ash subbituminous coal with CO2 activation." AIChE Journal 44(5): 1170.

Toles, C., W. Marshall and M. Johns (1997). "Granular activated carbons from nutshells for the uptake of metals and organic compounds." Carbon 35(9): 1407.

Tseng, R., S. Tseng and F. Wu (2006). "Preparation of high surface area carbons from Corncob with KOH etching plus CO2 gasification for the adsorption of dyes and phenols from water." Colloids and Surfaces A: Physicochemical and Engineering Aspects 279(8): 69.

Withby, C. (2010). Applied Microbiology and Molecular Biology in Oil Field Systems. New York, Springer.

Yalçın, N. and V. Sevinç (2000). "Studies of the surface area and porosity of activated carbons prepared from rice husks." Carbon 38(14): 1943-1945.

Yang, R. T. (2003). Adsorbents: Fundaments and application., New York, John Wiley & Sons Inc. ISBN: 9780471462415

Yang, T. and A. Lua (2006). "Textural and chemical properties of zinc chloride activated carbons prepared from pistachio-nut shells." Materials Chemistry and Physics 100(2-3): 438.

Zhang, A., Q. Ma, K. Wang, X. Liu, P. Shuler and Y. Tang (2006). "Naphthenic acid removal from crude oil through catalytic decarboxylation on magnesium oxide." Applied Catalysis A: General 303(1): 103-109.

Zhang , A.,Q. Ma, K. Wang, Y. Tang, W. A., Goddard, (2005). Improved Processes to Remove Naphthenic Acids. Final Technical Report; DOE: DE-FC26-02NT15383 California, California Institute of Technology.